FIZIKA

A JOURNAL OF EXPERIMENTAL AND THEORETICAL PHYSICS

Volume 4 — Supplement

Proceedings of the Meeting of Yugoslav Nuclear Physicists, Opatija, November 24–26, 1971

EUROPHYSICS JOURNAL

Published by the Commission for Physics of the Yugoslav Union of Mathematical and Physical Societies and the National Committee of IUPAP

The Meeting was sponsored by:

COUNCIL FOR SCIENTIFIC RESEARCH OF S. R. CROATIA, ZAGREB and INSTITUTE "RUĐER BOŠKOVIĆ", ZAGREB.

The Meeting was organised by: P. Tomaš and D. Rendić,
Department for Nuclear and Atomic Physics,
Institute "Ruđer Bošković".

The edition of this Supplement is financed by the Council for Scientific Research of S. R. Croatia and Institute "Ruđer Bošković", Zagreb.

This Supplement contains the invited and contributed papers reported at the annual Meeting of Yugoslav Nuclear Physicists, held in Opatija on November 24—26, 1971.

The papers are distributed in the groups according to the Sections in the Meeting programme. The papers submitted for publication in this Supplement have been reviewed by the undersigned members of the Editorial Committee.

Zagreb 15. 05. 1972.

D. Rendić
P. Tomaš
Z. Marić
R. Popić

FIZIKA 4 Suppl. (1972)

OPENING SESSION

Parity violation and nuclear forces

E. FISHBACH, *Purdue University, Lafayette*

D. TADIĆ, *Institute »Ruder Bošković«, Zagreb*

Although weak parity violating $\Delta S = 0$*) interactions among nucleons can provide us with many pieces of information which are unobtainable elsewhere, the study of this subject is a rather complicated undertaking. The accompanying box diagram intends to give a pictorial illustration of all theoretical steps, including doubts, uncertainties, and many-sided alternatives, which are necessary to produce results confrontable with experiments. The fact that only one box was allocated to the experiment, and that at the bottom of our scheme, reflects the fact that this paper intends to comment some aspects of the theory. Experimental papers reveal[1] that experimenting with $\Delta S = 0$ parity violating nuclear forces is no less intricate.

Even at the first step in the theoretical approach one is confronted with practically endless variety of possible models of weak interactions, which might, in fact, be just a first approximation to the »real« thing. Most of the common models, those od the »common type«[2], boil down to some or other current-current structure, and their consequences will be discussed at great length later on. For such models, the sign of the parity violating internucleon potential due to the ϱ-exchange contribution can be predicted provided that the intermediate-vector-boson field of positive metric mediates the weak interaction. That is the sign, which seems to disagree with the existing experiments. In the case when no intermediate boson field is exchanged, the current-current product can, obviously, have any sign. However, there is a third possibility[3], namely that intermediate vector bosons are of negative metric. In that case the sign of the ϱ-exchange contribution comes out to be opposite, so it would agree with experimental evidence. The investigation of other boxes in our diagram shows that such a statement, at this stage, cannot be taken too seriously. More has to be learned about two (or more) particle exchange contributions to the weak internucleon potentials, and nuclear physics problems have to be worked out in great detail. The experiments, which are still far from being perfected[1,4], will actually be testing theories involving both particle physics and nuclear physics hypotheses and assumptions. In order to make this somewhat

*) S is the strangeness. We will denote the isospin by T.

easier, one has to strive to experimentally distinguish parts of the potential with different isospin selection rules (i. e. $\Delta T = 1$ from $\Delta T = 0,2$). With some luck, in a few year time, the determination of the relative sign of the weak Fermi to electromagnetic coupling constant,[3] might be a discussable item.

Not much can in general be said on the unconventional models of weak interactions[2], such as in Ref.[5], as their consequences have not always been completely worked out. One can mention that the models of the Kummer-Segré type[6,7] attractive because being renormalizable, are already in trouble, as they allow, in a very natural way, for semiweak internucleon interactions, thus predicting for larger parity violating effects than observed experimentally. In order to forbid these semiweak contributions, they has to go into very inelegant contortions[7], predicting a whole array of new, yet unobserved, particles. The situation in weak interaction models is further complicated by some evidence originating from nuclear beta decay[8] which suggests that second-class currents[9] might be present.*)

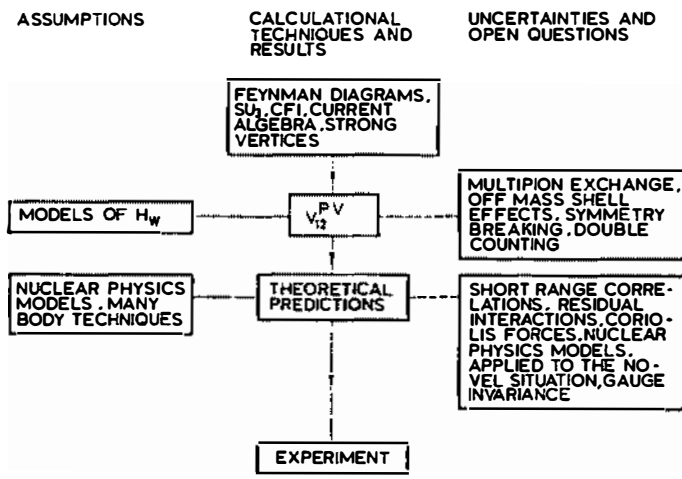

Such currents would naturally lead to the $\Delta T = 1$ contribution to the weak internucleon potential[13], whose general form is similar to the pion exchange contribution, but whose magnitude can be estimated only with difficulty[14]. In principle, such a contribution can either enhance the pion exchange effect, or destructively interfere with it.

In this communication we are first going to illustrate how the step from the weak Hamiltonian to the weak internucleon potential is made, discussing many of the difficulties involved. Once the potential is obtained, we have to discuss the problems connected with the gauge invariance, which are important when dealing with photon emitting processes. Some facets of nuclear physics calculations are investigated while going along the main line in our box diagram; others are only

*See, however, a recent study[10] (as well as papers[11,12]) where negative evidence is presented.

mentioned and referred to the other articles[15,16]. In the end some experimental evidence is explored attempting to draw some conclusions which can be based on the general features. In the above text, some of these possibilities have already been referred to.

References

1) P. Bock, Proceedings of the Zagreb Symposium 1971; E. Kuphal, M. Daum and E. Kankheleit, Proc. of the Zagreb Symposium 1971; V. M. Lobashov and L. M. Smotritski, Leningrad (1971) (preprint);
2) H. Pietschmann, Proc. of the Zagreb Symposium 1971.
3) T. D. Lee, Phys. Rev. Lett. **26** (1971) 801;
4) V. M. Lobashov and L. M. Smotritski, Leningrad (1971) preprint;
5) Y. Tanikawa and S. Watanabe, Phys. Rev. **113** (1959) 1344;
6) W. Kummer and G. Segré, Nucl. Phys. **64** (1965) 585;
7) N. Christ, Phys. Rev. **176** (1968) 1086;
8) D. H. Wilkinson, Physics Today (September 1970); Phys. Letters **31B** (1970) 447; **32B** (1970) 190; Phys. Rev. Lett. **24** (1970) 1134;
9) B. Kuchowicz, Acta Phys. Polon. **20** (1961) 341; B. Eman and D. Tadić, Glasnik Mat. Fiz. i Astr. **17** (1962) 81; J. N. Huffaker and E. Grenling, Phys. Rev. **132** (1963) 738;
10) J. Blomquist, Phys. Letters **35B** (1971) 375;
11) F. Krmpotić and D. Tadić, Phys. Rev. **178** (1969) 1804;
12) B. Eman and D. Tadić, Proc. of the Zagreb Symposium 1971;
13) R. J. Blin-Stoyle and P. Herezeg, Nucl. Phys. **B5** (1968) 291; Phys. Letters **23** (1966) 376;
14) D. Tadić, Phys. Rev. **174** (1968) 1694;
15) N. Vinh-Mau, Proc. of the Zagreb Symposium 1971;
16) H. Kümmel, Proc. of the Zagreb Symposium 1971.

FIZIKA 4 Suppl. (1972)

SECTION 1 — PARTICLE PHYSICS

1.1 High-energy scattering of an electron off a bound electron

M. MARTINIS, *Institute »Ruder Bošković«, Zagreb*

We consider a model in which the bound electron is viewed as an electron infinitely many times scattered off the external potential. The amplitude and the wave function may be found using the eikonal approximation, in which the internal momenta of the electron are replaced by

$$(p - \sum k_i)^2 - m^2 \cong 2p \sum k_i.$$

The model thus obtained gives a possibility to consider the scattering of very fast electrons or gamma quanta off an electron bound in the nucleus.

1.2. Electromagnetic form factors of pions and nucleons

Z. ZOVKO, *Institute »Ruder Bošković«, Zagreb*

Couplings of the existing and also of the still hypothetical vector mesons to nucleons and pions are calculated from the dispersion theory of form factors within the VMD model. The results are compared with the values obtained from vector meson contributions to the nucleon-nucleon potential.

Dynamical information is induced by asumptions on the high-energy behaviour of the form factors. Some suggestions about the masses of possible, still undiscovered, vector mesons are obtained. Form factors are calculated only in the spacelike region of the invariant momentum transfer. Finally, calculations are compared with the experimental data and the existing formulas following from dual models.

1.3. Some properties of the charged Σ hyperons*

D. N. TOVES and D. H. DAVIS, *Physics Department, University College London*

J. SIMONOVIĆ, *Institute of Physics, Beograd*

G. BOHM, J. KLAUBUHN and F. WYSOTZKY, *Institut für Hochenergiephysik, Berlin-Zeuthen*

M. CSEJTHEY-BARTH and J. H. WICKENS, *Université Libre de Bruxelles*

T. CANTELL, *Institute of Advanced Studies, Dublin*

C. NI GHOGAIN and A. MONTWILL, *Physics Department, University College, Dublin*

K. GARBOWSKA-PNIEWSKA, T. PNIEWSKI and J. ZAKRZEWSKI, *Institut of Experimental Physics, Warsaw*

A sample of some 7500 K^- meson captures at rest on hydrogen in emulsion giving rise to charged $\Sigma\pi$ pairs has been used to determine r, the decay branching ratio of the Σ^+ hyperon, γ, the ratio of Σ^- to Σ^+ hyperon productions, τ_{Σ^-}, the lifetime of the Σ^- hyperon, and C, the mean orbital capture time of Σ^- hyperons in emulsion. The results were

$$r = \frac{\Sigma^{\pm} n + \pi^+}{\text{all } \Sigma^+ \text{ decay modes}} = 0.484 \pm 0.015,$$

$$\gamma = \frac{\Sigma^- \pi^+}{\Sigma^+ \pi^-} = 2.34 \pm 0.08, \quad \tau_{\Sigma^-} = (1.41 \, {}^{+0.09}_{-0.08}) \cdot 10^{-10}\text{s}, \text{ and } C < 10^{-12}\text{s}.$$

1.4. Fragmentation of light nuclei in nuclear emulsion induced by 1.5 GeV/c K^- mesons

O. ADAMOVIĆ, M. JURIĆ and W. SIDIQUI, *Institute of Physics, Beograd*

The interaction of K^- mesons with heavy and light emulsion nuclei has been investigated in nuclear emulsion exposed to 1.5 GeV/c K^- mesons. The probability of interaction of K^- mesons with heavy and light nuclei is determined and compared to S values obtained by means of the optical model of interaction. An analysis is made of events of interaction on light nuclei in respect to the amount, mass and charge of emitted fragments and the excitation energy of the decaying residual nucleus. In particular, interactions leading to the emission of a hypernucleus are studied. The probability is determined of the emission of a hypernucleus in the interaction of 1.5 GeV/c K^- mesons with light emulsion nuclei, and the mechanism is discussed by which the hypernucleus emission takes place.

*Work published in Nuclear Physics **B33** (1971) 493—504.

1.5. Production of fact nuclei of A = 3 together with hypernuclei induced by 1.5 GeV/c K⁻ mesons on heavy nuclei*

Ž. TODOROVIĆ and M. JURIĆ, *Institute of Physics, Beograd*

In this work an analysis has been made of the production of helium nuclei and tritons of energy greater than 70 MeV in events with hypernuclei. The results of measurement of the helium nuclei show that the nuclei are predominantly ^{3}He. The energy spectra and angular distributions of ^{3}He nuclei and tritons are similar. The distributions of the total number of black and gray tracks (N_h) for events in which fast ^{3}He nuclei and tritons are emitted also are similar. These facts point out that the production mechanism of ^{3}He nuclei and tritons is the same. In events in which an $A = 3$ nucleus is emitted with energy higher than 200 MeV the number of detected cascade particles is lower than in events in which an $A = 3$ nucleus is emitted with an energy in the interval 70—200 MeV. This difference in the number of cascade particles is most likely due to different mechanisms of their production. In this work the production mechanisms of these nuclei are discussed. It is shown that fast nuclei of $A = 3$ most likely arise from the absorption of secondary π mesons and of the primary K^- meson in ^{4}He-clusters present in the outer regions of heavy nuclei.

1.6. $^8_2$He nuclei amongst hammer fragments in the interaction of K⁻ mesons with emulsion nuclei

S. POPOV and M. JURIĆ, *Institute of Physics, Beograd*

An investigation has been carried out on fragments of a charge $Z = 2,3$ and 5 with the characteristic decay into two alpha particles and one electron, the so-called hammers in the interaction of 10.1 and 1.5 GeV/c K^- mesons and of K^- mesons at rest with emulsion nuclei.

Using the method of measuring track width and detecting 2 electrons, fragments have been found belonging to $^8_2$He. The yield production of these fragments is determined.

Theoretical investigations[1,2] concerned with determination of the stability limits of light nuclei point to the possibility of the existence of $^8_2$He nuclei formed during rapid disintegrations of the heavy nuclei and emitted together with the fragments of different masses and charges.

There are two modes of decay proposed for the $^8_2$He nucleus:

$$\text{I} \quad {}^8_2\text{He} \xrightarrow{\beta^-} {}^8_3\text{Li}\ (0.978;\ 1^+) \xrightarrow{\gamma} {}^8_3\text{Li} \xrightarrow{\beta^-} {}^8_4\text{Be}\ (2.9;\ 2^+) \rightarrow 2\,{}^4_2\text{He}$$

$$\text{II} \quad {}^8_2\text{He} \xrightarrow{\beta^-} {}^8_3\text{Li}\ (3.22;\ 1^+) \rightarrow {}^7_3\text{Li} + \text{n}.$$

*Work published in Fizika 4 (1972) 77—85.

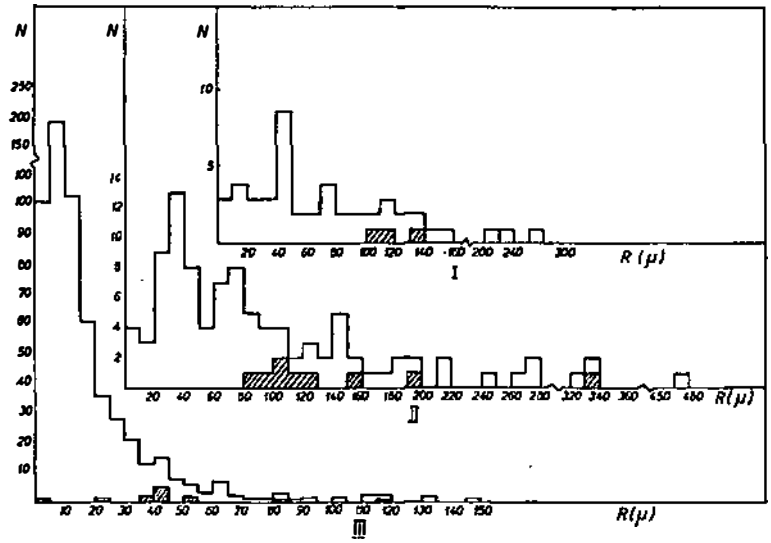

Fig. 1. The range distribution of hammer tracks in emulsions irradiated by:
I K^- 10,1 GeV/c,
II K^- 1,5 GeV/c,
III K^- low energy.

Acording to Paskanzer[3] et al. the probability of the first kind of decay is 88% for the second is 12%.

In nuclear emulsions, the first mode of the decay appears as a characteristic T-shape track, so called hammer, which is similar to those obtained for the $^{8}_{3}$Li and $^{8}_{5}$B nuclei. Such tracks can be separated determining the charge by the track-width measurement in the emulsion, or by the indentification pairs at the decay vertex. Several papers[4-7] have been published so far, with the aim to prove the existence of the ^{8}He and to find out the frequency of its apperarance. As the results obtained differ and the statistics is low, further work on this problem is still of interest.

TABLE 1

$P_{\bar{K}}$ GeV/c	Total stars investigated	HAMMERS							
		Found	Electron emission				Track width measurements		
			1 el		2 el		Number	With $z \simeq 2$	
0	262 783	616	511	83%	3	~0.5%	82	13	~16%
1.5	15 300	98	84	86%	1	~1%	71	9	~12.7%
10.1	6 660	45	35	78%	0	—	25	3	~12%

In the present paper the interaction of 10.1 GeV/c, 1.5 GeV/c K^- mesons and of K mesons at rest with the emulsion nuclei, has been investigated. The track of stars were analysed to separate the events with the $^{8}_{2}$He hammers.

Three stacks of Ilford G-5 emulsion were used in this analysis; the first was exposed to the K^- mesons beam of 10.1 GeV/c, the second to the K^- mesons beam of 1.5 GeV/c and the third to the K^- mesons at rest. The irradiation carried out at CERN.

Identification of the hammers was performed by investigations the T-shape tracks taking into account the presence of an electron at the decay vertex and measuring the widths of hammer tracks.

The tracks of all hammers were carefully examined to identify electron pairs at decay verteces. In order to identify Z hammers only those ones were selected which satisfied following criteria:

a) the projected range of the track should be $R > 20$ μm,

b) the dip in the processed emulsion should not exced 45°, and

c) the track should not lie within 25 μm from either surface of the emulsion.

The widths of the tracks were measured by a well known method also developed by us[8].

The results of measurements are given in Table 1.

The range distribution of hammer tracks is shown in Fig. 1. the shaded aerea correspondes to $^8_2$He.

Investigations and measurements on hammers led us to the following conclusion: The percentages of $^8_2$He nuclei found by the two methods show significant differences; therefore the proportion of $^8_2$He obtained by the electron pair identification method, ammounting to 0,5%, may be considered as the lower limit for the production rate.

TABLE 2

Authors	Primary particles	Number of hammers	Number of $^8_2$He	
Yu Batusov et al.	$\bar{u}^-$ at rest	7145	3	~0.04%
Cüer et al.	K^- 1.5 50 GeV/c P 25 GeV/c $\bar{u}^-$ 17 GeV/c $\bar{P}$ 5.0 GeV/c	1916	10	~0.5%
G. C. Deka et al.	$\bar{u}^-$ 3.5 GeV/c	348	7	~2%
M. Jurić et al.	K^- at rest	616	3	~0.5%

Our results are in good agreement with those found in the literature[5] (Table 2).

References

1) J. B. Zeldovič JETP 38 (1960) 1123;
2) A. J. Baz et al. YFN 85 (1965) 445;
3) A. M. Paskanzer et al. Phys. Rev. Lett. 15 (1965) 1030;
4) Yu. A. Batusov et al. OHRN Dubno (1966) E-2774;
5) G. Baumen et al. N. C. 51 B (1967) 483;
6) O. C. Deka, et al. N. C. 15 B (1966); 63
7) B. Bhownik et al. N. C. LIII A, N2, 400;
8) M. Jurić et al. N. C. B8 (1968) 565.

1.7. Final state interaction in the mesonic decay of hypernucleus ${}^{5}_{\Lambda}$He

B. DRAGOVIĆ, *Institute of Physics, Beograd*

1.8. Meson hyperfragments of A → 5 produced by the interaction of K^- mesons at rest in nuclear emulsions

M. JURIĆ, *Institute of Physics, Beograd*

Owing to the research carried out within the framework of the European K^- collaboration about 2700 meson hyperfragments (HF) with A > 5 have been studied. The better statistics and stricter selection criteria made it possible to determine more precisely the binding energies of the hyperons in HF. Thereby it has been stated that there is no hypernucleus ${}^{6}_{\Lambda}$Li, that ^{7}Li exhibits no exhausted states, which could not be stated for ${}^{7}_{\Lambda}$He, further the binding energies for several groups of mirror HF have been determined and compared, which makes it possible to study the symmetry violation with respect to charge in the interaction of λ hyperon with nucleons; a new HF, ${}^{10}_{\Lambda}$Be, has been discovered and so on.

Also the excited state of the hypernucleus ${}^{11,12}_{\Lambda}$C and the excitation energy have been determined.

FIZIKA 4 Suppl. (1972)

SECTION 2 — METHODS OF NUCLEAR PHYSICS

2.1. Application of the perturbated angular correlation method to the study of the magnetism

S. KOIČKI and A. KOIČKI, *Institute »Boris Kidrič«, Beograd*

2.2. Some problems of lifetime measurements with Doppler shift attenuation method

M. VAKSELJ, P. KUMP and P. RUPNIK, *Institute »Jožef Stefan«, Ljubljana*

2.3. The measurement of penetration profiles of Argon ions in Tantalum using (p, gamma) reaction

M. VAKSELJ, P. KUMP AND P. RUPNIK, *Institute »Jožef Stefan«, Ljubljana*

2.4. The unitary operator method in theory of slow neutron scattering by bound centers system

V. STANČIĆ *Institute »Boris Kidrič«, Beograd*

Abstract: An operator suitable for treating slow neutron scattering by a system of bound centers has been derived by starting from one general expression of the unitary operator in the scattering theory. A conection of the obtained operator with the Heisenberg number density operator has been shown. The expression of slow neutron scattering cross section expressed by the correlation function has been obtained for the first Born approximation. However, this method is useful for studing the number density function or the two-body potential. The proposed method has been applied to potential and resonance neutron scattering.

The intention of this work is to introduce the number density operator in the theory of nuclear reactions, whenever the interaction of incoming particle-bound center of the system may be described as a two body potential. Some informations about the number density, correlation function or the two body potential may be obtained by the interpretation of the experimental results. The use of this operator has been illustrated in the case of slow neutron scattering treating the potential and the resonance scattering.

Let the Hamiltonian of the whole system be

$$H = H_0 + V, \tag{1}$$

then the solution of the wave equation may be expressed using the unitary operator $U(t, t_0)$

$$| \alpha, t\rangle = U(t, t_0) | \alpha, t_0 \rangle \tag{2}$$

$$i\hbar \frac{\partial U(t, t_0)}{\partial t} = H(t)\, U(t, t_0) \tag{3}$$

$$U^+(t, t_0)\, U(t, t_0) = 1, \tag{4}$$

where $H(t)$ is the evolution operator:

$$H(t) = \exp(iH_0\, t/\hbar) V \cdot \exp(-iH_0 t/\hbar). \tag{5}$$

In the case of potential scattering the bound centers system is actually the system of atoms and the two-body potential takes the form of the Fermi potential[1,2,3])

$$V_1(\vec{r} - \vec{r}_l) = 2\pi a\hbar^2/m\delta(\vec{r} - \vec{r}_l), \tag{6}$$

or for the whole system

$$V(\vec{r}) = \sum_i V_1(\vec{r} - \vec{r}_l) = a_1 \sum_i \delta(\vec{r} - \vec{r}_l), \tag{7}$$

where m is the neutron mass and a-the scattering length. The evolution operator reduces into

$$H(t) = a_1 \varrho(\vec{r}_t, t), \tag{8}$$

where

$$\varrho(\vec{r}_t, t) = \sum_i \delta(\vec{r}_t - \vec{r}_i(t)) \tag{9}$$

is the number density operator. However, in the case of the resonance scattering the potential reduces to

$$V(\vec{r}) = \int d^3r' V_1(\vec{r}) \varrho(\vec{r} - \vec{r}', 0), \tag{10}$$

and the evolution operator (5) becomes

$$H(t) = \int d^3r' V_1(\vec{r}) \varrho(\vec{r}_t - \vec{r}', t). \tag{11}$$

By using the perturbation expansion of the operator $U(t, t_0)$ the transition matrix element in the first Born approximation becomes

$$\langle i | U_1(\infty) | f\rangle = -\frac{ia_1}{\hbar} \int d^3r dt \exp\left[i(\omega t - \vec{K} \cdot \vec{r})\right] \varrho(\vec{r}, t), \tag{12}$$

for the potential scattering. With the help of (12) the potential cross section takes the form of Van Hove's results. In the case of resonance scattering the matrix element

$$\langle i \mid U_1(\infty) \mid f \rangle \approx -\frac{i}{\hbar} \int \mathrm{d}^3 r' V_1(\vec{r}') \int_0^\infty \mathrm{d}t \exp\left[-i(\hbar\lambda_K - E_i)\, t/\hbar \cdot \right.$$

$$\left. \cdot \langle i \mid \Phi_K \rangle \langle \Phi_K \mid \varrho(\vec{r} - \vec{r}', 0) \mid f \rangle \sim \frac{\text{const}}{\hbar\lambda_K - E_i} \right. \tag{13}$$

is the usual Breit-Wigner expression[4,5,6].

The used number density function in (13) has been obtained by solving the Louville type equation

$$\frac{\partial \varrho}{\partial t} = \frac{i}{\hbar} \left[\varrho, H_0 \right] = -iL\varrho,$$

where $\hbar\lambda_K = E_0 - i\Gamma/2$ and Φ_K are the eigenvalue and eigenfunction of the non-hermitian operator L.

References

1) A. C. Zemach, R. J. Glauber, Phys. Rev. **101** (1956) 118;
2) L. Van Hove, Phys. Rev. **95** (1954) 249;
3) P. Schofield, Phys. Rev. Letters **4** (1960) 239;
4) H. Feshbach, Ann. of Phys. **5** (1958) 357;
5) C. Bloch, Nucl. Phys. **4** (1957) 503;
6) R. Jancel, »Foundations of Classical and Quantum Statistical Mechanics«, Oxford 1963

2.5. Gamma-ray planar Si(Li) polarimeter

V. KOS, K. ILAKOVAC, A. LJUBIČIĆ AND B. HRASTNIK, *Faculty of Electrical Engineering, Zagreb and Institute »Ruđer Bošković«, Zagreb*

Linear polarization is defined by the ratio

$$P = \frac{N_1 - N_2}{N_1 + N_2},$$

where N_1 and N_2 are the numbers of photons polarized in two mutually perpendicular directions.

Following the measurements of Honzatko and Kajfosz[1] and of Ewan et al.[2], a planar Si(Li) detector was applied as a polarimeter and its sensitivity determined. The beam of linearly polarized gamma rays was achieved by Compton scattering of 122 keV gamma rays from a 2 mCi source of ^{57}Co in graphite at 90°. Linearly polarized gamma rays undergo a second Compton scattering in the detector, preferentially in the plane perpendicular to the direction of polarization[3]. The number of pulses in the total energy peak for the two orientations of the detector (parallel and perpendicular to the polarization plane) were determined. From these results an asymmetry ratio $A = (3.0 \pm 0.6)\%$ was obtained[4].

A systematic investigation of planar Si(Li) polarization analyzers of different geometry and dimensions has been undertaken, and a new apparatus was built (Fig.) to improve the method of measurement. In this system the positioning of the detector and the scatterer on the axis of rotation can be accomplished to a better accuracy. A further improvement is the measurement of the number of pulses in four positions (two and two opposite positions for »parallel« and »perpendicular« measurement), which is expected to yield a practical elimination of systematic

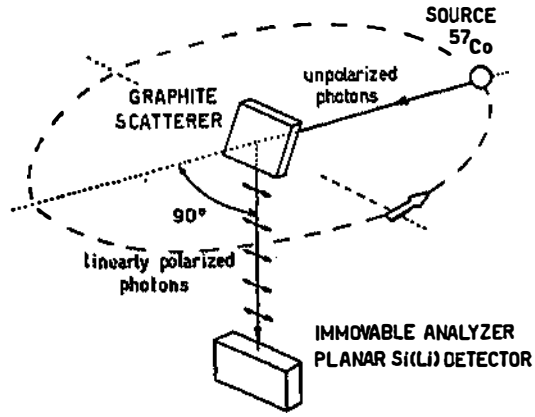

Fig. Schematic illustration of the polarimeter.

errors. The number of counts in the detector N, due to the variation of the scattering cross section in the graphite scatterer, is a function of the deviation x of the detector from the symmetry axis. The sum of numbers of counts in two opposite positions will be

$$N(x_1) + N(-x_1) = N(0) + N(0) + x_1 \frac{dN}{dx} - x_1 \frac{dN}{dx} + \frac{1}{2} x_1^2 \frac{d^2N}{dx^2} + \\ + \frac{1}{2} x_1^2 \frac{d^2N}{dx^2} + \dots .$$

The linear terms practically cancel and the quadratic and higher order terms are negligible.

In the new arrangement it is also easy to check whether the detector or the scatterer are in the proper position by comparing the number of pulses in the opposite positions. From this asymmetry one may draw conclusions about the eccentricity and the necessary correction of the position.

References

1) J. Honzátko and J. Kajfosz, Československa Akademie Ved, Report UJF 2113-F (1968), Czech. J. Phys. **B19** (1969) 1281;
2) G. T. Ewan et al., Phys. Lett. **B29** (1969) 352;
3) O. Klein and Y. Nishina, Z. Phys. **52** (1929) 853;
4) V. Kos et al., Planarni detektori kao analizatori polarizacije, V Kongres mat. fiz. i astr. Jugoslavije, Ohrid, 14—19. IX 1970.

2.6. Polarimetric efficiency of a planar Ge(Li) detector

B. MOLAK, K. ILAKOVAC and J. NOSIL, *Institute »Ruđer Bošković«, Zagreb*

Application of a single Ge(Li) planar detector[1,2] to measurements of the degree of linear polarization of gamma rays has some advantages over the coincidence spectrometers: it is simple and reliable and the detection efficiency is relatively high. The main disadvantage is a lower polarimetric efficiency.

An Ortec Ge(Li) planar detector of ϕ18 × 3 mm was used for measurements of linear polarization. Since the detector could not be rotated, a system was built by means of which the plane of polarization was rotated, other conditions being unchanged (see Fig.). To determine the polarimetric efficiency of the system for different gamma-ray energies, Compton scattering of 662 keV, 1173 and 1332 keV gamma rays was used. The degree of polarization of secondary Compton photons (P_C) obtained by scattering in graphite at a number of angles, was calculated. From the measured asymmetry of the counting rates $A = (N_1 - N_2)/(N_1 + N_2)$ the polarimetric efficiency $\varepsilon = A/P_C$ was calculated. N_1 and N_2 are the counting rates when the plane of polarization is parallel and perpendicular to the plane of the detector, respectively.

An approximate formula for the polarimetric efficiency has been derived

$$\varepsilon \approx F \cdot \frac{\mathrm{d}\sigma_C(E,\Theta)}{\mathrm{d}\Omega} \cdot P_C(E,\Theta)/\sigma_{tot}, \qquad (1)$$

where $\mathrm{d}\sigma_C/\mathrm{d}\Omega$ and P_C are the differential cross section and the degree of linear polarization of photons of incident energy E when scattered by the Compton effect at an angle Θ, for which the product is maximum, σ_{tot} is the total cross section for the absorption of gamma rays and F a normalizing factor. A comparison of the results of measurements and of the calculated values of ε_{th} is given in the Table on the p. 16.

References

1) J. Honzátko and J. Kajfosz, ČS Akad. Véd Report 2113-F (1968); Czech. J. Phys. B19 (1969). 1218;
2) G. T. Ewan, G. I. Anderson, G. A. Bartholomew and A. E. Litherland, Physics Letters 29B (1969) 352.

2.7. Tests and calibration of a 3D system

K. ILAKOVAC, M. JURČEVIĆ and B. MOLAK, *Institute »Ruđer Bošković«, Zagreb*

Multiparametric analysis of events has become a widely applied technique in complex experimental methods of investigation in nuclear physics. A three-dimensional (3D) system of 256 × 256 × 256 channels (24 bit) with the provision for extension up to 36-bit recording of data has been built in the Department of Electronics in the Institute. It is used in connection to a double- or triple-input fast-slow electronic system. Coincident data are analyzed in three ADC-s and the channel numbers recorded on punched paper tape. The total number of channels

TABLE

Polarimetric efficiency of planar Ge(Li) detectors.

E0(MeV)	0.233	0.288	0.382	0.475	0.570	0.660	0.847	1.368	1.779	4.43
$\varepsilon^{(a)}(\%)$	3.98±0.12	5.06±0.10	5.61±0.09	6.5±1.2	5.5±0.7	7.2±1.0				
$\varepsilon^{(b)}(\%)$	—	—	—	5.68±0.17	—	—	7.85±0.5	5.20±0.75	6.3±0.8	3.2±0.5
$\varepsilon^{(c)}(\%)$	4.37	4.95	5.65	6.03	6.21	6.26	6.26	5.82	5.27	2.53

a) our result with an ⌀ 18×3 mm detektor, increased by an estimated faktor of 1.1 for comparison. with results (b);
b) results of Ewan et al.[2], divided by a factor of 2 to have the same definition of asymmetry A;
c) values for $\Theta = 40°$ calculated from formula (1).

is extremely large and presents difficulties in the analysis of data. A programme for the analysis of double decay processes in the decay of nuclear levels has been written in the Real Time Fortran language for the off-line analysis of data in a CAE 9040 computer.

The system was electronically tested for linearity, time resolution, stability etc. For the measurements of a double gamma decay in which two coaxial Ge(Li) detectors were applied, a calibration of the system was made by Compton scattering of gamma rays from one detector into another. The time difference between the pulses from the two detectors was recorded in one channel and the amplitudes of the pulses in the other two channels. The calibration measurements yielded a straight line in the amplitude 1 — amplitude 2 diagram, since a continuous distribution of energy deposited in each detector was obtained (due to the variation of the scattering angle), with the condition of a constant sum. The same applied in the case of double decay. A detailed investigation of the time spectra (time dimension) along the constant sum line was made. When one amplitude increases the other decreases, and this causes shifts (of about 30 ns) of the time distributions. A considerable improvement of the time resolution was obtained when corrections for these shifts were introduced in the analysis of data, depending on the channel numbers of amplitude 1 and amplitude 2.

2.8. Automatic analysis of the gamma radiation spectra

I. SLAVIĆ, *Institute »Boris Kidrič«, Beograd*

2.9. The short dead time of halogen parallel plate counters

V. HENČ-BARTOLIĆ, *Faculty of Electrical Engineering, Zagreb*

Introduction. The investigation of properties of halogen (Ne-Br_2) parallel plate counters of the Srdoč type[1] revealed the possibility of constructing counters with a dead time shorter by an order of magnitude than that of cylindrical GM counters.

In general, the decrease of the impedance connected to the counter causes the reduction of the dead time. The dead time of parallel plate counters with low impedance (300 kΩ) and the pressure ratio $P_{Ne} : P_{Br2} = 100$ is short, less than 10 μs. In particular cases, if P_{Br2} is 1.2 torr and the distance between the electrodes 3 mm, the dead time is 6 μs.

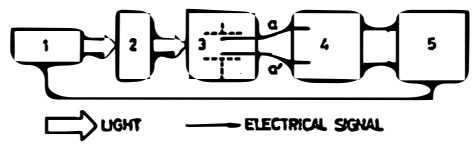

Fig. 1.

To explain this phenomenon, the discharge in the counter caused by gamma or beta particles was measured using the experimental setup described below.

Experimental setup. The setup used in the present measurement is shown in Fig. 1. The circuit with the discharge tube is labelled by (1). The optical system (2) produces the image (3) of the light pulse emitted between the electrodes. The light from two different spots of the image (3) is conducted by means of two plastic light guides »Crofon« (a and a') to the cathodes of two RCA IP28 photomultipliers (4). The photomultipliers are connected to an oscilloscope (Tektronix 551) through two cathode followers (4). The time bases of the scope are triggered by the voltage pulse from the discharge tube.

Measurements and conclusion. The described method is a suitable tool for investigating the place and time dependence of the discharge ($I = I(t, x)$.) It was observed that a low intensity light pulse near the anode appeared first, followed by a high intensity light pulse near the cathode (Fig. 2). The time delay between these two light maxima decreased with increasing electrode voltage. The time delay was of the order of 100 nsec.

The light guides used can transmit only wave lengths corresponding to the deexcitation of neon ($3p$—$3s$) levels.

Light pulses from the discharge tube indicated that the density of the space charge was increased near the anode. The U. V. emission of neon and bromine (for $\lambda < 275$ nm) caused the secondary emission of electrons at the cathode. The electrons thus produced gave rise to an intense development of new avalanches near the cathode, followed by an increase in density of the space charge in this range.

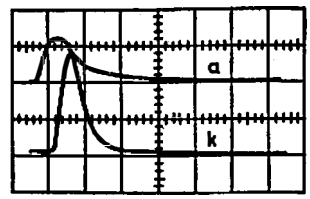

Fig. 2.

The dead time is defined by recombination of slow-mobility positive ions. In a cylindrical counter the discharge is developed mainly in the centre of the tube near the anode. The dead time of such a counter is longer in comparison with that of a parallel plate counter. One of the properties of the latter counter is that positive ions are concentrated near the cathode.

Reference

1) D. Srdoč: Nucl. Instr. and Meth. 21 (1963) 243.

2.10. Acceleration of nitrogen and neon ions to energies above 200 MeV/nucleon

K. PRELEC, *Institute »Ruđer Bošković«, Zagreb*

M. ISAILA and M. G. WHITE, *Princeton Particle Accelerator, Princeton, N. J., USA*

Until recently the scientific interest for heavy ions was more or less limited to energies below 10 MeV/nucleon. This range of energies was of special interest for nuclear physicists with their desire to explore problems of nuclear structure

or to try the synthesis of superheavy elements. In recent years biologists have made predictions that nitrogen or neon ions would be far superior to γ-rays in treating deeply situated malign tumors. Space biology has its own problem: radiation effects of the heavy component of cosmic rays on the nerve tissue of astronauts during long, planetary space trips. The energies involved in the latter two cases are up to 500 MeV/nucleon.

In the present state of the accelerator technology, synchrotron is the only accelerator capable of accelerating ions of any charge-to-mass ratio to energies up to and above 1000 MeV/nucleon. There are, however, a few additional requirements to satisfy. A R. F. accelerating system with a very wide range of frequencies is necessary and the vacuum in the vacuum chamber has to be good enough to avoid excessive losse due to a charge change of ions.

The synchrotron in Princeton, N. J., U. S. A., started to operate as a proton machine in 1963. Its basic parameters are: $B \cdot R = 12.8\,\mathrm{T} \cdot \mathrm{m}$, acceleration time $T = 25$ ms, vacuum $(1 - 2) \cdot 10^{-7}$ torr. In 1969 a program was initiated for the conversion of the synchrotron into a machine capable of accelerating any ion up to uranium, to energies of 1000 MeV/nucleon. The first phase of the project consisted in the acceleration of nitrogen and neon ions. The choice of the ion species was dictated by the need for the most suitable radiation in cancer treatment. In later phases of the project the replacement of the existing epoxy vacuum chamber with a ceramic one is envisaged; this would improve the vacuum down to 10^{-9} torr, necessary for ions heavier than neon.

The mode of acceleration of nitrogen and neon ions is as follows. From a compact Penning ion source a mixture of nitrogen or neon ions in different charge states is extracted, accelerated in a 4 MV Van de Graaff and then the 2+component separated in a B×E mass spectrometer. By passing through a carbon stripping foil of 10 $\mu g/cm^2$ thickness the mean charge in the beam is increased to 5—6. The desired species is again separated in an electrostatic analyzer, injected into the main synchrotron ring and accelerated to the final energy.

On July 15, 1971 nitrogen ions were accelerated to 290 MeV/nucleon. This was the first time that heavy ions of cosmic energies have been obtained in the laboratory. In September the energy was increased to 530 MeV/nucleon. The intensity of the external beam was up to $2 \cdot 10^6$ particles per second. At the same time a series of biological experiments was begun.

Note added. On December 15 a neon beam was obtained, with an energy of about 500 MeV/nucleon.

2.11. Study of the phosphorescent component of NaI(Tl) and possibility of its application

S. KOIČKI, A. KOIČKI and V. AJDAČIĆ, *Institute »Boris Kidrič«, Beograd*

2.12. The K-Shell fluorescence yields of argon, chlorine and sulphur

J. PAHOR, A. MOLJK, A. KODRE, T. RUPNIK and M. HRIBAR, *J. Stefan Institute, University of Ljubljana, Ljubljana*

The fluorescence yields of noble gases neon, argon, krypton and xenon were measured[1-7] by using the proportional counter. Recently, some modifications of the original method were introduced by which large corrections required previously

were reduced, and by which the method became applicable for measurement on other gaseous compounds not disturbing the normal operation of the proportional counter[8]. In the present work the similar experimental arrangement was utilized.

For measurement of fluorescence yield for argon the multiwire proportional counter was filled with 15 mm of mercury of argon, 40 mm of methane and with helium up to 760 mm. Fig. 1. represents a spectrum obtained by use of incident

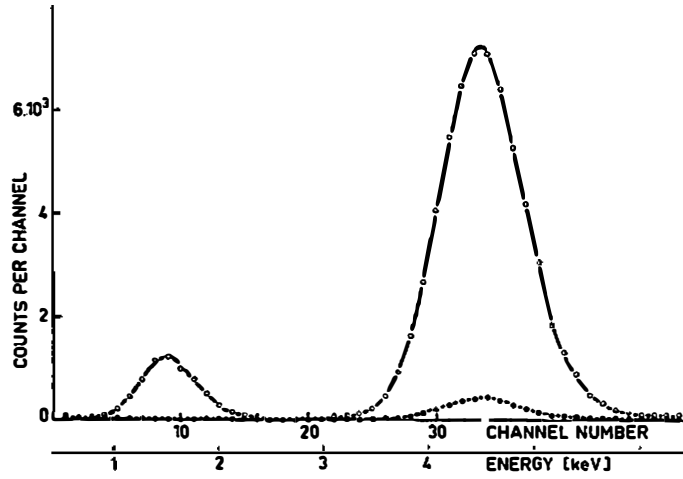

Fig 1.

radiation with energy $E_0 = 4{,}5$ keV from titanium target. The spectrum exhibits the main peak due to the Auger transition at energy E_0 and the escape peak at energy $E_0 - E_K$ due to the radiative transition with E_0 being the energy gap between K and L shells. The contribution to the spectrum due to the conversion of incident radiation in methane, determined separatelly, is represented in the same figure by the lower curve.

For determination of fluorescence yield of chlorine the methyl chloride CH_3Cl was used as converter. The partial pressure of methylchloride not interfering the normal operation of proportinal counter was found to be 5 mm of mercury in the absence of helium. Therefore only methane was added up to 65 mm of mercury. The spectrum is represented in Fig. 2.

As a convenient compound for measurement on sulphur the dimethylsulphide was found. In this case an energy difference between main and escape peak in the case of titanium target was too small for accurate separation of both peaks and the measurement was performed using potassium K—X radiation.

Gas filling was 10 mm of mercury of dimethylsulphide and 60 mm of mercury of methane. As in the case of chlorine the use of helium was not possible because of decreasing energy resolution. For background measurements two methyl groups in dimethylsulphide were replaced by two methane atoms thus yielding the total presure 80 mm of mercury of methane. A typical spectrum with sulphur escape peak is represented in Fig. 3.

From the obtained spectra the relative activities N_m and N_e of the main and the escape peaks, respectively, were determined. These values have to be corrected for the escape of the electrons from the main counter and for the reabsorption of K fluorescent radiation of the investigated element. For the evaluation of ω_K the

fraction $N_e/(N_e + N_m)$ with corrected values of relative activities has to be divided by the absorption efficiency of the K shell, determined by the K jump values[9].

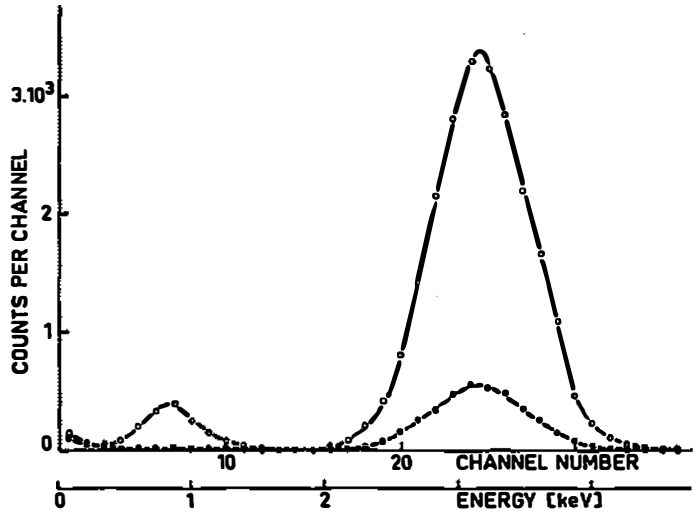

Fig. 2

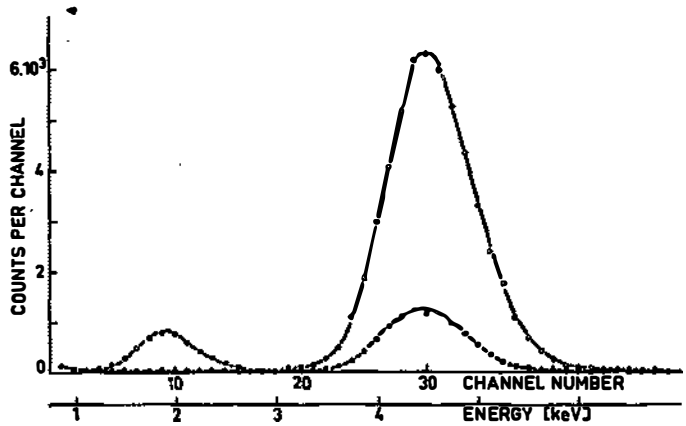

Fig. 3.

Thus for the fluorescence yields the following values result: for argon $(12{,}3 \pm 0{,}3) \cdot 10^{-2}$, for chlorine $(10{,}0 \pm 0{,}3) \cdot 10^{-2}$ and for sulphur $(8{,}2 \pm 0{,}3) \cdot 10^{-2}$.

References

1) J. Heintze, Z. Phys. **143** (1955) 841;
2) W. F. Frey, Phys. Rev. **113** (1959) 1057;
3) Hanna, Kahn see West in Frish Progress in Nucl. Phys. **3** (1953) 43;
4) G. Bertolini, A. Bisi and L. Zappa, Nuovo Cim. **10** (1953) 1424;
5) G. R. Harrison, Phys. Rev. **100** (1955) 841;
6) D. West and P. Rothwell, Phil. Mag. **41** (1950) 873;
7) G. M. Insch, Phil. Mag. **41** (1950) 857;
8) J. Pahor, A. Kodre and Moljk, Nucl. Phys. **A109** (1968) 62;
9) M. A. Blohin, Fizika rentgenovskih lučej, Moskva 1957.

2.13. Study of internal fields in $BiFeO_3$ by Mössbauer spectroscopy

D. HANŽEL, M. MALI and A. MOLJK, *J. Stefan Institute, University of Ljubljana, Ljubljana*

The antiferromagnetic-ferroelectric ferrite $BiFeO_3$ with weak ferromagnetic properties[1] was studied by Mössbauer efect[2] in the temperature range from 8° — 760°K. The measured spectra show bellow the Neel temperature $T_N = 643$°K six line distribution characteristic for a strong magnetic hyperfine interaction while above the Neel temperature T_N have two peaks shape typical for quadrupole interaction.

At 9°K spectrum yields the internal magnetic field of 548 ± 10 KG, isomer shift relative to metallic iron of 0.56 ± 0.05 mm/sec and quadrupole splitting of 0.42 ± 0.05 mm/s. The values above 90°K agree with the results published recently by Biran et al.[3]

The angle Θ between the electric field gradient and the direction of the internal magnetic field can be estimated on the base of Kunding[4] analysis as 80°—90°. The Morin transition induced by the turning of the electron spins over 90° has not been observed down to 8°K.

Molecular field approximation with the Brillouin function for $S = 5/2$ and $H_0 = 550$ KG fits the experimental values for relative internal magnetic fields in the range 8°K — 640°K, while the spin wave T^2 approximation is satisfying in the range bellow 260°K. Both approximations lead to the same value for the exchange integral $|J|k^{-1} = 36.7$.

With the value determined for quadrupole splitting $\Delta E = 0.38 \pm 0.04$ mm/s at 670°K and with the assumed quadrupole moment for iron in 14,4 keV state $Q = 0.41$ barn[5], the field gradient results as $V_{zz} = 9.1 \pm 0.2 \cdot 10^{17}$ V/cm^2.

Using the reported data of unit cell obtained by the electron diffraction[5] analysis the components of electric field gradient have been calculated by the point charge lattice sum with the Wette-Schacher[7] planewise method. Result is axially symmetric electric field gradient with the principle exis $V_{zz} = 4.3 \cdot 10^{16}$ V/cm^2 paralel to the threefold (111) axis. The disagreement between the calculated and the measured value could be explained by the uncertainty of the positions of ions and of the quadrupole moment and by the neglect of the covalent bonding effect at iron ion. The latest data[1,8] for the positions of ions at 600°C bring calculated value for V_{zz} closer to the measured one which indicates strong dependence of V_{zz} for changes in ion parameters in the lattice.

References

1) C. Michel, J. M. Moreau, G. D. Achenbach, R. Gerson and W. J. James, Solid State Commun. **7** (1969) 701;
2) D. Hanžel, A. Moljk, Report IJS — DP-306, 1970;
3) A. Biran, P. A. Montano, U. Shimony, J. Phys. Chem. Sol. **32** (1971) 327;
4) W. Kunding, Nucl. Inst. and Meth. **48** (1967) 219;
5) J. O. Artman, Phys. Rev. **143** (1966) 541;
6) Ju. Ja. Tomaspolskij, Ju. I. Venevcev, G. S. Ždanov, Dokl. A. N. SSSR **153** 6 (1963) 1313;
7) F. W. De Wette and G. E. Schacher, Phys. Rev. **137** (1965) A92
8) J. M. Moreau, C. Michel, R. Gerson and W. J. James, J. Phys. Chem. Sol **32** (1971) 1315.

2.14. An internal rotating target for the cyclotron

T. LECHPAMMER and B. BABAROVIĆ, *Institute »Ruđer Bošković«, Zagreb*

The technical description of an internal rotating target for the 16-MeV cyclotron of the »Ruđer Bošković« Institute is given. The target has been designed in such a way that its bearing housing is mounted on a plate-shaped cover, similarly as in stationary targets.

The holder of the target is a brass tube of an outer diameter of 25 mm. The target is shaped like a hollow disk and is placed at one end of the holder. The middle part of the holder passes through the housing and rotates together with it. The end of the target holder passes through a double cooling chamber. Cooling water is supplied to the target by an inner tube and is sent back through the body of the holder itself. Rotational motion is transmitted to the target from an electromotor by two pairs of gears, the speed of rotation being approximately 80 rotations per minute.

The rotating target is in principle made of the material to be bombarded. Another possible way of making the target is to pour the metal to be bombarded into a hollow in the standard copper target.

The rotating target has the advantage of permitting bombardment of material with a low melting point, applying currents that are higher by a factor of 2—3 than in the case of stationary targets.

Measurements of the beam current impinging on the rotating target can be performed by calorimetric and electric methods. Measurements by the former method are performed in a similar manner as in stationary targets, i. e., by reading out the differences in temperature of the cooling water at the outlet and the inlet.

To perform measurements by the latter method, the target should be grounded by a low-pass filter (to eliminate high frequencies at the target) and by a terminal resistor. The electric voltage obtained across this resistor by the ionic beam current is fed to a recorder which gives an indication corresponding to the beam intensity.

FIZIKA 4 Suppl. (1972)

SECTION 3 — NUCLEAR STRUCTURE

3.1. Solving the many-body problem with linear programing

M. V. MIHAILOVIČ and M. ROSINA, *Institute »Jožef Stefan«, Ljubljana*

3.2. Quadrupole moments of the even-even vibrational nuclei

G. ALAGA, F. KRMPOTIĆ, V. LOPAC, V. PAAR and L. ŠIPS, *Institute »Ruđer Bošković«, Zagreb*

Recent measurements of the quadrupole moments in the even-even vibrational nuclei have provided a good test for different nuclear models. The purpose of the present report is to extract the main effects responsible for the existence of the quadrupole moment and to compare the mechanisms provided by different types of approach.

In analogy with the polarization effect observed in the odd-proton nuclei, such as Sb, In, etc., where the large ground-state quadrupole moment was explained by coupling one particle to the harmonic vibrator

$$Q(j)=Q_{s.p.}(j)\left[e_{\mathrm{eff}}^{p}+\frac{5}{4\pi}Ze\frac{\langle k\rangle}{C}\right],$$

one expects a similar process for two or more particles coupled to the vibrator[1,2,3]. However, in going from the one- to the two-particle case, a qualitatively new feature, i. e., the short-range residual force between the two particles, is encountered.

The quadrupole moment of a two-particle 2^+ state is given as

$$eQ(2_1^+)=Q[(j)^2 2]\cdot\left[e_{\mathrm{eff}}^{p}+\frac{5}{4\pi}Ze\frac{\langle k\rangle}{C}\right], \tag{1}$$

exhibiting the same polarization effect as in the one-particle case. However, in a vibration nucleus the 2_1^+ state is of the one-phonon rather than of the two-particle type due to the large energy gap Δ separating the paired from the broken pair states. In this case both the zeroth and first order contributions vanish. The lowest nonzero particle and vibrational contributions are of second and third order, giving the result

$$eQ(2_1^+)=Q_{s.p.}[(j)^2 2]\left[e_{\mathrm{eff}}^{p}+\frac{5}{4\pi}Ze\frac{\langle k\rangle}{C}\right]\cdot x^2(j),$$

which is identical to (1) except for the last factor including the energy denominators. The corresponding diagrams are shown in Fig. 1.

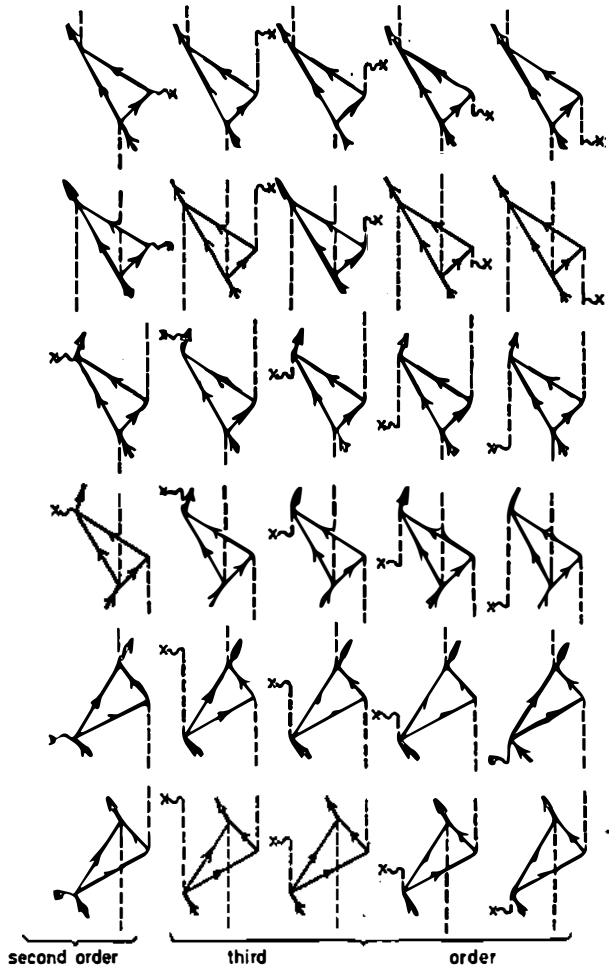

Fig. 1.

If several configurations are available, the effect is the same, but the sum has to be taken over all intermediate particle states.

The semimicroscopic result can be connected with that obtained in the phenomenological anharmonic model[2,4]. If the third-order terms of the type $\sim A_1 b^+ b^+ b$ are added to the harmonic Hamiltonian, the quadrupole moment becomes, in the first approximation,

$$eQ(2_1^+) = \sqrt{\frac{16\pi}{5}} \begin{pmatrix} 2 & 2 & 2 \\ -2 & 0 & 2 \end{pmatrix} \left(\frac{3}{4\pi} Ze \sqrt{\frac{\hbar\omega}{2C}} R_0^2 \right) (-4 A_1). \qquad (2)$$

The nature of the phenomenological constant A_1 can be understood by searching for the quasi-particle excitations building the phonon. The diagrams corresponding to (2) are shown in Fig. 2. Comparison with Fig. 1 shows that the semimicroscopic model is more complete, because it includes processes with the explicit presence of particles.

Both the semimicroscopic and the anharmonic model quadrupole moment can be written in the following form:

$$eQ(2_1^+)=Ke_{\mathrm{eff}}^M\sum_{jj'j''}\langle j''\|Y_2\|j\rangle\langle j\|Y\|j'\rangle\langle j'\|Y\|j''\rangle\begin{Bmatrix}2&2&2\\ j&j''&j'\end{Bmatrix}D^M(jj'j'')\,U^M(jj'j'') \tag{3}$$

where M denotes the model-dependent quatities e_{eff}^M, D^M and U^M which characterize the effective charge, the energy denominators and the occupation probabilities of the particle orbits, respectively. Essentially the same form (3) is obtained in the pairing + quadrupole study of the vibrational nuclei[5].

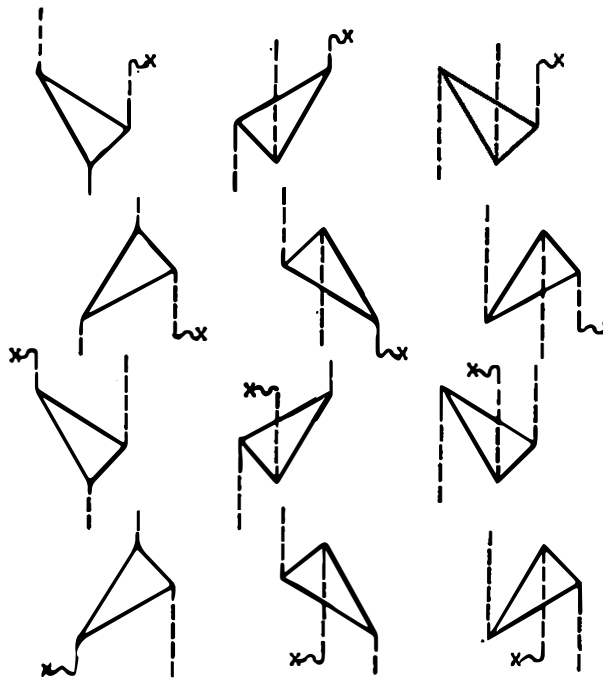

Fig. 2.

Expression (3) shows that the structure of the 2_1^+ state is strongly affected by the particle properties in spite of the apparently vibration-like character of this state. The competition of different configurations will determine the sign of the total quadrupole moment. Generally, terms with nondiagonal matrix elements have a sign opposite to the sign of terms containing diagonal elements. For two particles coupled to the vibrator the diagonal terms are positive and the nondiagonal

TABLE

Nucleus	Available proton configurations	Dominant matrix element		Quadrupole moment		
		Diagonal	Nondiagonal	A	Exper.	Theory (semimicroscopic)
$_{56}$Fe	$f_{7/2}^{-1}$	$\langle f_{7/2}^{-1} \| Y_2 \| f_{7/2}^{-1} \rangle$	—	56	—0.22	—0.21
$_{80}$Hg	$s_{1/2}^{-1}, d_{3/2}^{-1}, h_{11/2}^{-1}, d_{5/2}^{-1}$	—	$\langle s_{1/2}^{-1} \| Y_2 \| d_{3/2}^{-1} \rangle$	198	—	0.83
$_{51}$Te	$g_{7/2}, d_{5/2}, s_{1/2}, d_{3/2}, h_{11/2}$	$\langle g_{7/2} \| Y_2 \| g_{7/2} \rangle$	$\langle g_{7/2} \| Y_2 \| d_{3/2} \rangle$	122 124 126 128	—0.50 —0.40 —0.27	—0.08 +0.07 —0.01
$_{48}$Cd	$g_{9/2}^{-1}, p_{1/2}, p_{3/2}, (f_{5/2}^{-1})$	$\langle g_{9/2}^{-1} \| Y_2 \| g_{9/2}^{-1} \rangle$	$(\langle p_{1/2}^{-1} \| Y_2 \| f_{5/2}^{-1} \rangle$	114	—0.38	—0.37 —0.18 —0.33

negative. The opposite holds for holes. Whatever the result of this shell effect is, it is always enhanced several times due to the coherence of the particle and vibrational contributions.

This basic mechanism is valid in both models. The discrepancy in the results should be attributed to the model-dependent quantities and to the choice of the subspace over which the sum in (3) is taken.

For illustration the Table gives the dominant diagonal and nondiagonal proton matrix elements as well as some characteristic experimental and theoretical values for some isotopes with two protons or two proton holes in the closed shell. In such cases the two proton cluster imposes its motion to the whole nucleus and is almost entirely responsible for the existence of the nonzero quadrupole moment. More details of the calculations as well as references on experiments are given in Ref. 6.

References

1) A. Bohr and B. R. Mottelson, Nuclear Structure II, W. A. Benjamin, New York;
2) G. Alaga, Proc. International School in Theoretical Physics, Predeal 1969;
3) V. Lopac, Ph. D. Thesis, Zagreb 1971;
4) L. Šips and V. Lopac, Phys. Lett. **32B** (1970) 649;
5) L. S. Kisslinger and R. A. Sorensen, Rev. Mod. Phys. **35** (1963) 853;
6) G. Alaga, V. Paar, R. A. Broglia, R. Liotta and V. Lopac, Nucl. Phys.;
V. Paar, Nucl. Phys., **A185** (1972) 544;
V. Lopac, Nucl. Phys., **A155** (1970) 513.

3.3. Application of the »bootstrap« on the states and processes around the doubly closed shell nuclei. The Pb case

R. A. BROGLIA, *The Niels Bohr Institute, University of Copenhagen, Copenhagen, Denmark and Institute for Theoretical Physics, State University of New York, Stony Brook, New York, USA*

B. NILSSON, *NORDITA, Copenhagen, Denmark*

S. LANDOWNE, *The Niels Bohr Institute, University of Copenhagen, Copenhagen, Denmark*

V. PAAR, *The Niels Bohr Institute, University of Copenhagen, Copenhagen, Denmark and Institute »Ruđer Bošković«, Zagreb, Yugoslavia*

D. R. BÈS, *CNEA, Buenos Aires, Argentina*

E. FLYNN, G. IGO and P. D. BARNES, *Los Alamos Scientific Laboratory, Los Alamos, USA*

A unified picture is developed to describe the situation around a closed shell nuclear system[1-8]. This approach is based on the diagrammatic method[1-3], accounting for the dominant processes, in particular for those states which are strongly excited in the (t, p), (p, t) reactions and/or inelastic scattering processes. In the shell-model language these are the 2p, 2h and 1p—1h states (pairing and surface vibrational states), and those generated by coupling these states among themselves (two-phonon states).

The bootstrap study was carried out in three successive steps:

i) the calculation of the elementary modes of excitation, i. e. the low-lying states, of each spin λ and parity $(-)^{\lambda}$. The residual forces which are diagonalized are multipole particle-hole and pairing interactions[2,5-7]. The only free parameters

entering in the calculation are the coupling constants $\varkappa(a = 0, \lambda, \tau)$ and $G(a = \pm 2, \lambda, \tau)$ which are fixed by fitting the experimental energy of the lowest state of each family of levels.

ii) The calculation of the coupling between the particles (holes) and the vibrational modes, i. e. the calculation of the admixture of 1p-states and 2p−1h states. The coupling strength between the particle (hole) and the vibration is fixed self-consistently by the value of the coupling constants determined in step i).

iii) The calculation of the interaction between the two-phonon states of ^{208}Pb. This interaction is built out of a series of particle-vibration vertices, and consequently the magnitudes of the different matrix elements are fixed self-eonsistently by the values of the coupling strengths obtained in step (ii).

In this way an effective interaction between the elementary modes of excitation as well as composed states is obtained. Particularly, the interaction between the $J^\pi = 0^+$ states was calculated and the results compared with the ^{206}Pb(t, p) and ^{210}Pb(p, t) reaction data [5,8]. The effective interaction between the states of two-phonons with $J_R = 2^+$ in ^{208}Pb is also constructed. Special attention was paid to the states $|2_1^+(^{206}\text{Pb}) \cdot \text{gs}(^{210}\text{Pb}); 2\rangle$ and $|\text{gs}(^{210}\text{Pb}) \cdot 2_1^+(^{210}\text{Pb}); 2\rangle$, and the predictions are compared with the reaction data. For the first time the result provides a clear evidence on the existence of isovector quadrupole mode which dramatically renormalizes (screens) the quadrupole interaction between particles and holes.

The ^{208}Pb(t, p) ^{210}Pb(3^-) reaction is analyzed in the coupled channel Born approximation (CCBA)[4,8]. The competition between the effects of the effective interaction, the effective transfer operator and two-step processes was evidenced.

The (t, p) cross section cannot be explained without accounting for the contributions due to the correlations induced in the ^{208}Pb ground state by the 0^+ pairing vibration and the 3^- particle-hole mode. The inclusion of indirect reaction channels which interfere with the direct one brings the improved results in closer agreement with experiment. The importance of these two effects is due to the collect ivity of the pairing and particle-hole modes in ^{208}Pb and ^{210}Pb, respectively.

References

1) A. Bohr and B. R. Mottelson, Nuclear Structure, Vol. II, W. A. Benjamin, New York;
2) D. R. Bès and R. A. Broglia, Phys. Rev. **C3** (1971) 2349; **C3** (1971) 2389;
3) V. Paar, Nucl. Phys. **A164** (1971) 576; **A164** (1971) 593; **A166** (1971) 341;
4) R. A. Broglia, S. Landowne, V. Paar, B. Nilsson, D. R. Bès and E. Flynn, Phys. Lett **36B** (1971) 541;
5) R. A. Broglia, V. Paar and D. R. Bès, Phys. Lett. **37B** (1971) 159;
6) R. A. Broglia, V. Paar and D. R. Bès, Phys. Lett. **37B** (1971) 257;
7) R. A. Broglia, V. Paar and D. R. Bès, Nucl. Phys.;
8) E. E. Flynn, G. J. Igo, R. A. Broglia, S. Landowne, B. Nilsson and V. Paar, Nucl. Phys. **A195** (1972) 97

3.4. On the BCS and HFB methods in terms of reduced density matrices

J. HENDEKOVIĆ, *Institute »Ruder Bošković«, Zagreb*

The basic assumption of the BCS model of spherical nuclei, which are characterized by a large number (10—20) of particles outside the inert core of doubly

closed shells, such as Sn isotopes, is that the ground state of a given nucleus may be described by the function[1] (expressed in the occupation number representation)

$$|\,\mathrm{BCS}\rangle = \prod_{\alpha>0}(u_\alpha + v_\alpha\, s_\alpha\, c_\alpha^+ c_{-\alpha}^+)\,|\,0\rangle, \qquad u_\alpha^2 + v_\alpha^2 = 1. \tag{1}$$

The above function is a mixture of components corresponding to all even systems possible in given orbits

$$|\,\mathrm{BCS}\rangle = \sum_{n=\text{even}} a_n\,|\,\psi_n\rangle, \qquad \sum a_n^2 = 1. \tag{2}$$

where $|\,\psi_n\rangle$ are special seniority zero states of the nucleus with n valence particles.

Thus, the $|\,\mathrm{BCS}\rangle$ function cannot be interpreted as a wave function of the given nucleus with N_0 valence particles. The central idea of this report is that the $|\,\mathrm{BCS}\rangle$ function can be interpreted as a convenient parametrization of the two-body reduced density matrix[2,3]

$$\varrho^{(2)}_{\alpha\beta\gamma\delta} = \langle \mathrm{BCS}\,|\,c_\alpha^+ c_\beta^+ c_\delta c_\gamma\,|\,\mathrm{BCS}\rangle. \tag{3}$$

In fact, this assumption is implicit in the standard BCS model, but there the one-body reduced density matrix is defined independently of (3) as

$$\varrho^{(1)}_{\alpha\beta}(\mathrm{BCS}) = \langle \mathrm{BCS}\,|\,c_\alpha^+ c_\beta\,|\,\mathrm{BCS}\rangle, \tag{4}$$

while it should be more consistently derived from (3) using the exact relation

$$\varrho^{(1)}_{\alpha\beta} = \frac{1}{N_0 - 1}\sum_\gamma \varrho^{(2)}_{\alpha\gamma\beta\gamma} \tag{5}$$

which gives

$$\varrho^{(1)}_{\alpha\beta} = \frac{1}{N_0 - 1}\langle \mathrm{BCS}\,|\,c_\alpha^+ c_\beta\,(N-1)\,|\,\mathrm{BCS}\rangle\,. \tag{6}$$

Taking the trace of relation (6), we arrive at the condition

$$\langle\,\mathrm{BCS}\,|\,N(N-1)\,|\,\mathrm{BCS}\,\rangle = N_0\,(N_0 - 1) \tag{7}$$

instead of the usual BCS condition $N_0 = \langle\,\mathrm{BCS}\,|\,N\,|\,\mathrm{BCS}\,\rangle$.

The above definition of the $\varrho^{(1)}$ matrix leads to some correction terms in the BCS gap equations. Numerical analysis shows that in most cases, when the standard BCS procedure works well, these correction terms do not change the results appreciably. However, for some forces, such as the Gaussian potential of Wigner type, for which the standard BCS procedure completely breaks down giving the unphysical energy much lower than the exact one, the above modification works as well as with other »good« forces. The reasons for this improvement may be traced down by careful analysis of the variational principle.

The more general HFB method can be modified in the same way, but additional problems appear when both neutrons and protons are considered. It seems that instead of the additional condition for the isospin

$$\mathrm{Re}\,\langle \mathrm{HFB}\,|\,T^2\,|\,\mathrm{HFB}\,\rangle = T(T+1), \tag{8}$$

the following (somewhat weaker) condition might turn out more useful

$$\mathrm{Re}\,\langle \mathrm{HFB} \mid N_n N_p \mid \mathrm{HFB} \rangle = N_n N_p. \tag{9}$$

In describing the excited states by the quasiparticle method based conceptually on ideas of reduced density matrices and transition amplitudes, a very consistent definition of spurious states can be reached which for higher excitations basically differs from the usual one.

References

1) M. Baranger, Phys. Rev. **120** (1960) 957;
2) P.-O. Löwdin, Phys. Rev. **97** (1955) 1474;
3) C. Garrod and J. K. Percus, J. Math. Phys. **5** (1964) 1756.

3.5. Investigation of the low energy spectrum in ^{93}Nb*

M. KREGAR, *Institute »Jožef Stefan«, Ljubljana* and G. G. SEAMAN *Kansas State University, Manhattan, Kansas, USA*

3.6. Projection of angular momentum from the generator coordinate wave function

N. MANKOČ-BORŠTNIK and M. V. MIHAILOVIČ, *Institute »Jožef Stefan«, Ljubljana*

3.7. Pairing vibrational states in Pb and Sn isotopes**

D. JUSTIN, M. V. MIHAILOVIČ and M. ROSINA, *Institute »Jožef Stefan«, Ljubljana*

3.8. A formula to calculate particle-hole excited states if the two-body density matrix of the ground state is known

M. ROSINA and M. V. MIHAILOVIČ, *Institute »Jožef Stefan«, Ljubljana*

3.9. Three-particle states in the semimicroscopic model

G. ALAGA and V. PAAR, *Institute »Ruder Bošković«, Zagreb, Yugoslavia, University of Zagreb, Yugoslavia* and *The Niels Bohr Institute, University of Copenhagen, Copenhagen, Denmark*

In nuclei with three particles (holes) away from a single-closed shell or a good subshell, the model of coupling a three-particle (hole) cluster to the quadrupole vibrational field was introduced in order to include the anharmonic structure of the neighbouring even nuclei as well as additional states based on broken and promoted pairs.[1-5] So far this model has been successfully applied to ^{51,53,55}Mn[5], ^{65,67,69}Ga[5], ^{107,109}Ag[5], ^{123,125,127}I[5] and ^{193,195,197,199}Au[1-4]. The success of the model is reflected in reproducing the global structure and the properties of the ground and excited states; this means that the overall agreement with experiment for low lying states is rather good (energy spectra, B(E2) and B(M1) values, electric

* Published in Nucl. Phys. **A179** (1972) 153—160.
** See Nucl. Phys. **A182** (1972) 54—68.

quadrupole and magnetic dipole moments, spectroscopic factors etc.), appreciably better than in other models (core-excited model, Kisslinger-Sorensen model, one particle coupled to a vibrator etc.). In addition, there are some experimental effects which are directly connected with a three-particle cluster:

i) the $I = j - 1$ anomaly for the ground state of ^{51,55}Mn ($5/2^-$) and ^{127}I ($5/2^+$) and for the lowest excited positive parity states in ^{107,109,111}Ag ($7/2^+$)[5],

ii) the positive quadrupole moment of the ground state and at the same time large spectroscopic factors of low-lying states in ^{64,67,69}Ga[5],

iii) the explicit appearance of the new negative parity states in ^{107,109}Ag in the region of a two-phonon multiplet[5],

iv) the complete breaking of the core-excitation intensity rules in ^{107,109}Ag[5], the corrected zeroth-order selection and intensity rules (CZOSIR)[4] etc.

References

1) G. Alaga, Bull. Am. Phys. Soc. **4** (1959) 359;
2) G. Alaga and G. Ialongo, Nucl. Phys. **A93** (1967) 481;
3) G. Ialongo, Ph. D. Thesis, New York University, 1966;
4) G. Alaga and V. Paar, Nucl. Phys.;
5) V. Paar, Phys. Lett., **39B** (1972) 466; **39B** (1972) 587; Nucl. Phys.

3.10. HRPA effects in even-even nuclei (microscopic and phenomenological approach)

G. DUSSEL, *CNEA, Buenos Aires, Argentina*

R. LIOTTA, *The Niels Bohr Institute, University of Copenhagen, Denmark*

R. A. BROGLIA, *The Niels Bohr Institute, University of Copenhagen, Copenhagen, Denmark and Institute for Theoretical Physics, State University of New York at Stony Brook, New York, USA*

V. PAAR, *The Niels Bohr Institute, University of Copenhagen, Copenhagen, Denmark and Institute »Ruder Bošković«, Zagreb, Yugoslavia*

In the particle-vibration coupling model[1], the leading order phonon-phonon interaction is given by rectangular and two-triangle diagrams[2]. The contributions from diagrams which appear in the adiabatic limit are calculated for the quadrupole vibrator. In this way, the strengths of quartic and cubic anharmonicities are expressed in terms of an underlying shell-model structure[2].

The leading-order contributions to the static quadrupole moments of the lowest $J^\pi = 2^+$ states in Ni, Sn and Pb isotopes have been calculated in the framework of a graphical perturbation method[3]. The microscopic structure of the 2^+ phonons is explicitly taken into account and the Pauli principle is respected up to the order of perturbation in which the quadrupole moments are calculated[3].

It was shown that the properties of an anharmonic vibrator follow the behaviour of the leading order processes, and thus are qualitatively simply determined by the coupling strengths of the anharmonic terms[4]. The Bohr collective Hamiltonian was solved analytically in the $\beta-\gamma$ representation and compared

with the contributions from the dominant diagrams[4]. The importance of quartic anharmonicities was also stressed, even for the strength of an order of magnitude smaller than for cubic terms. Especially important appear to be the interference terms. The dominant patterns of our analysis for the anharmonic structure of one- and two-phonon states are summarized in a kind of approximate intensity rules.

References

1) A. Bohr and B. R. Mottelson, Nuclear Structure II, W. A. Benjamin, New York;
2) V. Paar, Nucl. Phys. **A166** (1971) 341;
3) R. A. Broglia, R. Liotta and V. Paar, Phys. Lett., **38B** (1972) 480;
4) G. Dussel, R. A. Broglia and V. Paar, Nucl. Phys.

SECTION 4 — SIMPLE PARTICLE SYSTEMS

4.1. Study of three particle reactions on light nuclei induced by 14.4 MeV neutrons

B. ANTOLKOVIĆ, *Institute »Ruđer Bošković«, Zagreb*

Neutron induced breakup processes on some light elements have been studied in kinematically complete experiment. The correlation measurement has been performed by use of nuclear emulsions. In addition to the much higher yield which is allowed by the 4 π detection geometry, the measurements performed by this technique include also events extended to the whole momentum space. This seems to be of great importance for the study of the reaction mechanism.

The experimental data of the correlation spectra of $n+{}^{7}Li \rightarrow n+\alpha+t$ and $n+{}^{10}B \rightarrow t+\alpha+\alpha$ are presented in Dalitz diagrams. The analysis of contributions of different reaction mechanisms has been performed and data on some particle unstable states extracted. The spectra have been fitted with the Phillips, Griffy and Biedenharn theory for the sequential decay via $t-\alpha$, $n-\alpha$ and $\alpha-\alpha$ two particle states. It has been found that in both reactions studied, the contribution of the simultaneous breakup process is less than 10% of the total reaction crosssection.

4.2. Four-body break-up $d + {}^{11}B \rightarrow 3a + n$ and states in ${}^{9}Be$*

D. RENDIĆ and V. VALKOVIĆ, *Institute »Ruđer Bošković«, Zagreb*

N. D. GABITZSCH, W. von WITSCH and G. C. PHILLIPS, *Rice University, Houston, USA*

The four-body break-up of $d+{}^{11}B$ system into $3\alpha+n$ has been studied in order to obtain information about the decay properties of the excited states in ${}^{9}Be$. Experiment was performed using the tandem Van de Graaff accelerator and existing TOF facilities at Rice University, Houston, Texas. $\alpha-\alpha$ and $\alpha-n$ coincidences have been measured simultaneously at two bombarding energies 10.425 and 12.0 MeV.

Measured spectra reveal the importance of sequential decay mechanisms in the reaction; the process of the type

* Published in Nucl. Phys **A178** (1971) 49—59.

$$d + {}^{11}B \rightarrow \alpha_1 + {}^{9}Be_{2.43} \rightarrow \alpha_1 + \alpha_2 + {}^{5}He \rightarrow 3\alpha + n$$

is the most favoured one.

The decay structure of low-lying levels in ^{9}Be is discussed with regard to the n + ^{8}Be and α + ^{5}He clustering; while the 2.43 MeV state decays preferably to the α + ^{5}He$_{g.s.}$, 3.03 MeV state shows purely n + ^{8}Be$_{g.s.}$ decay structure. Decay properties of 4.70, 6.66 and 7.94 MeV levels are also studied.

4.3. Three-body break-up in the reaction d + ^{7}Li → α + α + n

J. HUDOMALJ, V. VALKOVIĆ and P. TOMAŠ, *Institute »Ruđer Bošković«, Zagreb*

The reaction d + ^{7}Li → α + α + n has been studied at deuteron bombarding energy E_d = 180 keV, with a target of natural lithium fluoride. The electronic set-up used is a standard slow-fast coincidence arrangement which enables a simultaneous measurement of α − α and α − n coincidence.

The experimental results show an evidence of a sequential decay mechanism of the reaction, through the ^{8}Be first excited state (2.9 MeV) and the ground state of ^{5}He. The coincidence spectra have been analyzed with the Breit-Wigner resonant term and the $\varrho^{1}(E_{rel})$ density of states function of Phillips-Griffy-Biedenharn. However, in both cases the shape of the spectra can be reproduced only approximately. In order to approve the agreement between the experimental and theoretical curves, a contribution of the direct three-body break-up has to be included, with lower limit of 5%.

4.4. The effect of the quasifree scattering process on the shape of kinematically incomplete spectra at forward angles in the deuteron breakup*

Ž. BAJZER and G. PAIĆ, *Institute »Ruđer Bošković«, Zagreb*

In the deuteron breakup the quasifree scattering (QFS) process appears alongside the final state interaction process (FSI) even at low incident energies. In the measurement of the D(n, p) 2n reaction at forward angles with single counter, the proton spectra should include both the effects of n−p and of n−n QFS. The n−n QFS effect on the spectra is limited to very low proton energies. The n−p QFS effect at small proton angles of detection overlaps kinematically with the location of the enhancement due to the FSI.

We present a preliminary calculation of the proton spectrum which has been performed taking into account only the n−p QFS in the D(n, p) 2n reaction for $\Theta = 0°$. A simple impulse approximation has been used at this stage. The result shows a marked maximum at high proton energies. The importance of the QFS effect for the extraction of the n−n scattering length is discussed.

---

* Work published in Fizika 4(1972) 113—120.

4.5. Study of the $^{12}C(n, n)3a$ reaction in a kinematically complete experiment

Z. DOLENEC and B. ANTOLKOVIĆ, *Institute »Ruđer Bošković«, Zagreb*

The reaction $n + {}^{12}C \rightarrow n + \alpha + \alpha + \alpha$ was investigates using nuclear emulsions simultaneously as a target and the detector. The reaction involves four particles in the final state; however the measurements of the three exit particles completely define the kinematics of the final channel. The three alpha prong events were measured and selected from other three prong processes in nuclear emulsion by the energy and momentum balance with the aid of an off-line CAE 90—40 computer code.

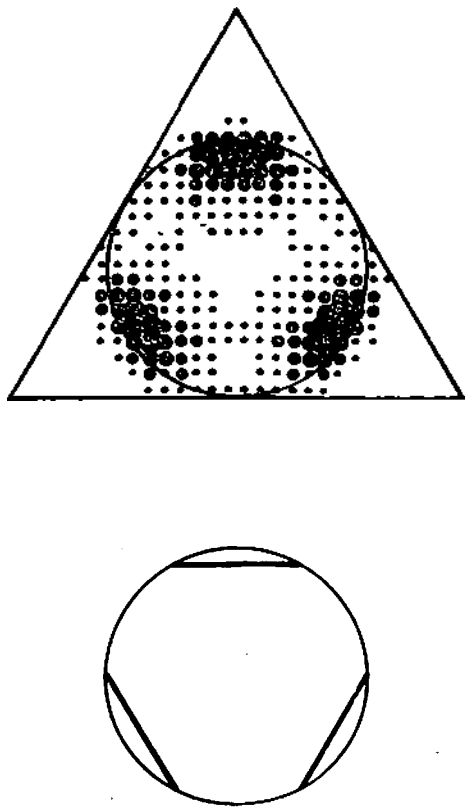

Fig. 1. Dalitz diagram of the three alpha breakup of the ^{12}C nucleus in the 9.6 MeV state. The loci of relative energies corresponding to the ground state of ^{8}Be are given in the lower scheme.

The neutron and alpha particle spectra in the ^{13}C centre-of-mass system as well as the spectrum of the n-alpha relative energies were analysed in order to define the contribution of different sequential processes:

1) $n + {}^{12}C \rightarrow n + {}^{12}C(\alpha)\,{}^{8}Be(2\alpha)$,
2) $n + {}^{12}C \rightarrow \alpha + {}^{9}Be(n)\,{}^{8}Be(2\alpha)$
   $\rightarrow \alpha + {}^{9}Be(\alpha)\,{}^{5}He(\alpha n)$, and
3) $n + {}^{12}C \rightarrow {}^{8}Be(2\alpha) + {}^{5}He(\alpha n)$.

It was found that the $^{12}C(n, \alpha)^{9}Be(n)2\alpha$ reaction contributes only in the intermediate 2.43 MeV state of ^{9}Be. The presence of this reaction manifests as a distinct peak on the continuum of the three alpha energies generated in the process 1) The intensity of the sequential process via ^{9}Be is 9.8%, but due to the kinematical conditions it coincides only with the events of process 1) involving ^{12}C excitations higher than 11.5 MeV.

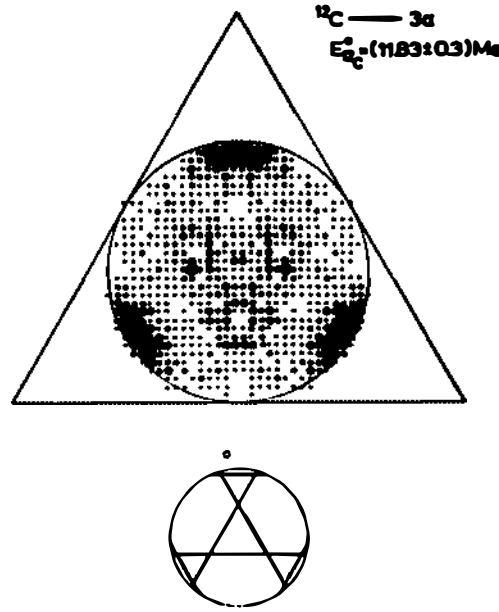

Fig. 2. Dalitz diagram of the three alpha breakup of the ^{12}C nucleus in the 11.8 MeV state. The loci of relative energies corresponding to the ground and first excited state of ^{8}Be are given in the lower sheme.

The overwhelming decay mode was found to be the $^{12}C \rightarrow 3\alpha$ chain of the process 1). The neutron energy spectrum exhibits a shape which is in accordance with the known level scheme of the ^{12}C nucleus. Hence the three correlation spectra were analysed for several ^{12}C resonances. Figs. 1 and 2 are representative Dalitz diagrams of the $^{12}C \rightarrow 3\alpha$ breakup involving the 9.6 and 11.8 MeV states of the ^{12}C nucleus.

The density distribution of the experimental data in Fig. 1 clearly demonstrates a sequential decay through the $^{8}Be_{g.s.}$ with the strong intensity peaks near the maximum energies of the three alphas. There is no trace of evidence for the simultaneous breakup to be present.

The data on the three alpha breakup of the 11.8 MeV state of ^{12}C nucleus presented in Fig. 2 show a high density of events along the lines corresponding to the transition via the ground state of ^{8}Be. A large part ($\sim$25%) of the ^{12}C(11.8 MeV) $\rightarrow 3\alpha$ decay process via the $^{8}Be_{g.s.}$ (0^+) contradicts the tentative 2^- spin-parity assignment[1], leaving 1^- as the only possible one. The spectrum also shows a very weak intensity of experimental points at the intersections of the two bands of the 2.9 MeV relative energies of ^{8}Be. These minima can be explained by the destructive interference effects.

References

1) F. Ajzenberg-Selove and T. Lauritsen, Nucl. Phys. A114 (1968) 1.

4.6. The three-nucleon bound state wave function from elastic electron scattering

N. BIJEDIĆ, *Institute »Boris Kidrič«, Beograd*

The theoretical investigation of the three-nucleon bound state wave function had a considerable success in the last few years. Nevertheless, the number of independent experimental data is less than the number of parameters we need to define the theoretical problem.

The cross section of the elastic electron scattering (defined as a product of Mott scattering cross section and the form factor of the nucleus) on ^{4}He and ^{3}He nuclei shows a diffraction minimum[1,2] in the region of squared momentum transfer $q^2 \sim 11(\text{fm})^{-2}$.

These data are explained as the efect of the repulsive core in the two nucleon interaction to the three and four nucleon bound state wave function [3,4,5]. In the case of the three-nucleon bound state wave function situation somewhat complicates

TABLE

$q^2(\text{fm})^{-2}$	$F_s(q^2)$	$F_{s-s'}(q^2)$
0	1.0000	0.0000
1	0.6497	—0.2029
2	0.4228	—0.2500
3	0.2768	—0.2351
4	0.1810	—0.1997
5	0.1175	—0.1611
6	0.0752	—0.1262
7	0.0469	—0.0971
8	0.0279	—0.0738
9	0.0152	—0.0555
10	0.0068	—0.0415
11	0.0013	—0.0308
12	—0.0023	—0.0227
13	—0.0045	—0.0166
14	—0.0057	—0.0121
15	—0.0064	—0.0087
16	—0.0066	—0.0061
17	—0.0065	—0.0043
18	—0.0063	—0.0030
19	—0.0059	—0.0020
20	—0.0054	—0.0013

by the presence of the higher symetry states, but for our purpose we can disregard D-state (see for example Ref. [4,5]) and charge form factor reads

$$F_{ch}(^3He) = \left(F^p_{ch} + \frac{1}{2}F^n_{ch}\right)(P^2_s F_s + P^2_{s'} F_{s'}) - \frac{1}{2} P_s P_{s'}(F^p_{ch} - F^n_{ch})_{s-s'} \quad (1)$$

$$F_{ch}(^3H) = (F^p_{ch} + 2F^n_{ch})(P^2_s F_s + P^2_{s'} F_{s'}) + P_s P_{s'}(F^p_{ch} - F^n_{ch}) F_{s-s'} \quad (2)$$

where the integrals F_s and $F_{s-s'}$ are given in Ref.[4] and in the Table, while $F_{s'}$ is given in Ref.[4] and is unimportante.

By direct inspection of the relations (1) and (2) and Table, one deduces the following conclusions:

1) for $P^2_{s'} = 0$, the diffraction minimum apears at $11(\text{fm})^{-2} < q^2 < 12(\text{fm})^{-2}$ for both ^3H and ^3He nuclei.

2) for $P^2_{s'} = 0.02$, the diffraction minimum is pushed back in q^2 for ^3He nucleus at $10(\text{fm})^{-2} < q^2 < 11(\text{fm})^{-2}$ and apears at $12(\text{fm})^{-2} < q^2 < 13(\text{fm})^{-2}$ for ^3H nucleus.

It is clear that the precise measurement of diffraction minimum for ^3H nucleus will determine the $P^2_{s'}$.

References

1) R. F. Frosh et al, Phys. Rev. **160B** (1967) 874;
2) J. S. McCarthy et al, Stanford HELP july 1970;
3) N. Bijedić and Z. Marić, L. Nouvo Cimento **2** (1969) 831;
4) N. Bijedić, Z. Marić and V. Zlatarov, Fizika **3** (1971) 11;
5) N. Bijedić, Ph. D. thesis, University Beograd 1970.

4.7. Preliminary report about the work on $^6He + ^1H$

R. POPIĆ, B. STEPANČIĆ and D. STANOJEVIĆ, *Institute »Boris Kidrič«, Beograd*

The cross-section of $^1H(^6He, t)^4He$ reaction is determined for $E_{^6He} = 0 - 5$ MeV by irradiating CH and CH_2 targets with ^6He particles obtained from the primary reaction $^7Li(t, ^6He)^4He$. The relatively large differential cross section of 0.7 b/sr is explained by low Coulomb barrier and a probable two-neutron correlation.

4.8. $^6Li(t, p)^8Li$ reaction at low energies*

D. ĆIRIĆ, B. STEPANČIĆ, M. ALEKSIĆ, R. POPIĆ, D. STANOJEVIĆ and K. SUBOTIĆ, *Institute »Boris Kidrič«, Beograd*

* Work published in FIZIKA 4 (1972) 193.

4.9. Some problems with separable potentials*

H. OBERHUMMER AND H. ZINGL, *Institut für Theoretische Physik, Universität Graz*

In a former work reported at the Symposium on the Nuclear Three Body Problem, Budapest 1971 we treated $^1S_0$ p—p scattering with a rank two potential of the form:

$$V(p', p) = \lambda_1 g_1(p') g_1(p) + \lambda_2 g_2(p') g_2(p),$$

where

$$g_1(q) = \frac{1}{q^2 + \beta^2}$$

$$g_2(q) = \frac{q^2}{(q^2 + \bar{\beta}^2)^2}.$$

We fit the parameters with the phase shifts[1] and find:

$\bar{\beta} = 1{,}2540$ fm^{-1} $\qquad \lambda_1 = -0{,}5442$ fm^{-2}

$\beta = 3{,}2992$ fm^{-1} $\qquad \lambda_2 \to \infty$

and get a badness of fit value $\chi^2 = 289$.

If we take $\lambda_2 = 0$ (usually called the Yamaguchi potential[2]), we obtain:

$\beta = 1{,}1538$ fm^{-1}
$\lambda_1 = -0{,}3760$ fm^{-2}
$\chi^2 = 760$.

The improvement by taking into account the repulsive core is considerable.

If the badness of fit value is not exactly equal to our best value, but within 10% deviation the rank 2 potential still is much better than Yamaguchi. So we could take also a finite λ_2, f. i. $\lambda_2 = 12{,}2$ fm^{-2}, then we obtain for the other parameters:

$\beta = 1{,}2440$ fm^{-1} $\qquad \lambda_1 = 0{,}5033$ fm^{-2}

$\bar{\beta} = 2{,}3601$ fm^{-1} $\qquad \chi^2 = 321$.

We denote this set as the λ_2-set.
The other three parameters can be varied in both directions to get the same badness of fit value. For instance we found:

β set:	$\beta = 1.2537,\ 1.2543$ fm^{-1}	$\lambda_1 = -0.5442$ fm^{-2}
	$\beta = 3.2992$ fm^{-1}	$\lambda_2 \to \infty$
$\bar{\beta}$ set:	$\beta = 1.2540$ fm^{-1}	$\lambda_1 = 0.5442$ fm^{-2}
	$\beta = 3.3083,\ 3.2880$ fm^{-1}	$\lambda_2 \to \infty$
λ_1 set:	$\beta = 1.2540$ fm^{-1}	$\lambda_1 = -0.5437,\ -0.5447$ fm^{-2}
	$\beta = 3.2992$ fm^{-1}	$\lambda_2 \to \infty$.

* Work supported by the Österreichischer Forchungsrat, Projekt 1211.

The parameters β, $\bar{\beta}$ and λ_1 are quite insensitive to small (10%) variations in χ^2 except λ_2, which changes drastically.

In the $^3S_1$ state, there is also the tensor force. This was investigated by many authors with the ansatz of Yamaguchi[3]. But these ansatz gives no polarization in N—N scattering[4]. One way to get out of this trouble is to use again a rank two potential of the form:

$$V(p', p) = \lambda_1 g_1(p') g_1(p) + \lambda_2 g_2(p') S(\hat{\vec{p}}) g_2(p) S(\hat{\vec{p}})$$

where the form factors g_1 and g_2 are given before and S is the usual tensor-operator. The parameters of this potential will also be fitted.

References

1) M. H. McGregor, R. A. Arndt and R. M. Wright, Phys. Rev. **182** (1969) 1714;
2) Y. Yamaguchi, Phys. Rev. **95** (1954) 1628;
3) Y. Yamaguchi and Y. Yamaguchi, Phys. Rev. **95** (1954) 1635;
4) H. Lambacher, Ph. D. Thesis, University of Graz.

4.10. Analysis of the off mass shell-behaviour of the hadronic scattering matrix as constructed by means of an effective Lagrangian model*

L. PITTNER and P. URBAN, *Institut für Theoretische Physik, Universität Graz, Austria*

Abstract: Starting from an effective Lagrangian model relativistic covariant and gauge invariant scattering amplitudes for certain hadronic interactions with an additional emitted or absorbed photon are constructed, which allow one to examine the validity of this Lagrangian model for off mass shell-hadrons.

Lagrange function for some hadrons and introduction of the photon. In this work a dynamical model for some hadrons is developed, which is based on an interaction Lagrangian for the pion nucleon system[1]. This Lagrange function includes the relativistic fields of the mesons σ ($J = 0^+$, $I = 0$), π and ϱ, the nucleons n and p and the baryon resonance $\Delta(1238)$ ($J = {}^3/_2{}^+$, $I = {}^3/_2$):

$$L_{int}(x) = g_{\sigma\pi\pi}\,\sigma(x)\frac{\vec{\pi}^2(x)}{2} + g_{\sigma NN}\,\bar{N}(x)\,N(x)\,\sigma(x) + g_{\varrho\pi\pi}\,\vec{\varrho}^{\mu}(x)\,[\pi(x)\times\partial_\mu\vec{\pi}(x)] +$$

$$+ g_{\varrho NN}\,\bar{N}(x)\,\gamma_\mu\frac{\vec{\tau}}{2}N(x)\,\vec{\varrho}^{\mu}(x) + g_{NN\pi}\,\bar{N}(x)\,\gamma_\mu\gamma^5\vec{\tau}\,N(x)\,\partial^\mu\vec{\pi}(x) +$$

$$+ g_{\Delta N\pi}\bar{N}(x)\,\vec{\tau}\,N_\mu(x)\,\partial^\mu\vec{\pi}(x).$$

* Supported by the Fonds zur Förderung der wissenschaftlichen Forschung in Österreich.

Now the principle of minimal electromagnetic coupling is used to introduce the relativistic photon field.

Scattering amplitude. The Lagrange function as developed above enables one to construct a relativistic covariant and completely gauge invariant scattering amplitude for certain hadronic processes with an additional absorbed or emitted photon. This electromagnetic interaction is regarded only to first order.

Of course the arising scattering amplitude contains the original purely hadronic scattering amplitude as kernel, but not all the hadrons, which this kernel is consisting of, are lying on the mass shell. This fact allows one to examine the validity of the underlying dynamical hadron model for off mass shell-handrons.

The resonance $\Delta(1238)$ is described in this model by a Feynman propagator which has a pole at the resonance position $S = M_\Delta^2$, where S is the squared four momentum of the Δ resonance. Therefore an imaginary part must be added to the resonance mass M_Δ in order to get finite cross sections. This can be done by the following standard method of field theory: the line of the internal Δ is replaced by the following Feynman graph

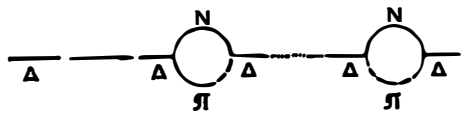

The corresponding scattering amplitude shows the right threshold behaviour too.

Special examples, parameters and results. To examine this Lagrangian model numerically two special scattering processes, which are connected by the crossing principle, are calculated explicitely:

radiative pion-nucleon scattering $\pi^+ p \to \pi^+ p\gamma$
double-pion photoproduction $\gamma p \to p\pi^+\pi^-$.

In these computations the following numerical values of the masses, coupling constants and corresponding decay widths of the involved particles are used:

$$m_\pi = 139.6 \text{ MeV}, \; M = 938.6 \text{ MeV},$$

$$M_\Delta = 1238 \text{ MeV}, \; m_\rho = m_\sigma = 765 \text{ MeV};$$

$$\frac{g^2_{\sigma\pi\pi}}{4\pi} = 67.4\, m_\pi^2 \; (\Gamma_{\rho\to\pi\pi} = 400 \text{ MeV}), \frac{g^2_{\sigma NN}}{4\pi} = 0.06,$$

$$\frac{g^2_{\rho\pi\pi}}{4\pi} = \frac{g^2_{\rho NN}}{4\pi} = 2.5 \; (\Gamma_{\rho\to\pi\pi} = 130 \text{ MeV}),$$

$$\frac{g^2_{p n\pi}}{4\pi} = \frac{0.08}{m_\pi^2},$$

$$\frac{g^2_{\Delta++\, p\pi}}{4\pi} = 18.6\, (\Gamma_{\Delta^{++}\to p\pi^+} = 120 \text{ MeV}).$$

With the above value of the coupling constant $g_{\sigma NN}$ the S-wave scattering length of elastic pion-nucleon scattering agrees with the experimental value

$$a_s^{(+)} = -\, 0.009\, m_\pi^{-1} \text{ [2]}.$$

For radiative pion-nucleon scattering the only experimental value so far known is[3]:

$$\sigma_{tot}(p\pi^+ \to p\pi^+\gamma) = 0.22 \pm 0.05 \text{ mb}$$

$$\text{at } E_{KIN}^{LAB}(\pi^+) = 300 \pm 70 \text{ MeV}.$$

In this case the results of the Lagrangian model[4] are lying too high, for example

$$\sigma_{tot}(p\pi^+ \to p\pi^+\gamma) = 0.55 \text{ mb} \qquad \text{at } E_{KIN}^{LAB}(\pi^+) = 300 \text{ MeV}.$$

But for the photoproduction $\gamma p \to p\pi^+\pi^-$ the predictions of the Lagrangian model[5] agree rather well with experimental data[6,7,8] for photon laboratory energies up to about 650 MeV.

Some remarks on the application of the Low-theorem on radiative pion-nucleon scattering. One very interesting feature of processes as for example radiative pion-nucleon scattering, which could be proved numerically by this work, is the following: The dependence of differential cross sections on the photon energy, as calculated by means of the Lagrangian model under discussion, shows explicitely, that it is not reasonable to analyse radiative processes, which are dominated by resonances as the $\Delta(1238)$, by means of the Low-theorem for soft photons, as done for example in[9], because the presence of such a strongly marked resonance as $\Delta(1238)$ disturbs the $1/K$ behaviour of cross sections (photon energy K)[10].

General conclusions. Up to now it is not clear, if the discrepancy between experimental data and the predictions of this Lagrangian model for pion-nucleon bremsstrahlung stems from the neglect of any possible momentum dependence of the coupling constants, or if this one experimental value is too small and should be corrected.

But for all the scattering processes, which have been discussed in this short survey, there are characteristic differences between the results of this non-unitary Lagrangian model and experimental data, which have their deeper reason in the fact, that there exists up to now no satisfactory relativistic quantum theory of unstable particles as for example the resonances of strong interaction.

References

1) B. Dutta-Roy, I. R. Lapidus and M. J. Tausner, Phys. Rev. **177** II (1969) 2529;
2) K. Raman, Phys. Rev. **164** (1967) 1736;
3) V. E. Barnes et al., CERN REPORT 63—27, Track Chamber Division, 22 July 1963;
4) R. Baier, L. Pittner and P. Urban, Nucl. Phys. **B27** (1971) 589;
5) L. Pittner and P. Urban, Nucl. Phys. **B39** (1972) 227;
6) B. M. Chasan, G. Cocconi, V. T. Cocconi, R. M. Schechtman and D. H. White, Phys. Rev. **119** (1960) 811;
7) J. V. Allaby, H. L. Lynch and D. M. Ritson, Phys. Rev. **142** (1966) 887;
8) A. Piazza, G. Susinno et al., Nuovo Cim. Lett. **III**, (1970) 403;
9) C. Picciotto, Phys. Rev. **185** II (1969) 1761;
10) H. Feshbach and D. R. Yennie, Nucl. Physics **37** (1962) 150.

SECTION 5 — NUCLEAR SPECTROSCOPY

5.1. Isotopic spin in photonuclear reactions*

G. KERNEL, *Institute »Jožef Stefan«, Ljubljana*

5.2. Photo-nuclear reaction cross sections for different decay channels on ^{90}Zr

D. BRAJNIK, D. JAMNIK, G. KERNEL, V. MIKLAVŽIĆ and A. STANOVNIK, *Institute »Jožef Stefan«, Ljubljana*

5.3. Parity nonconservation in heavy nuclei and the structure of weak-interaction hamiltonians**

B. EMAN and D. TADIĆ, *Institute »Ruđer Bošković«, Zagreb and University of Zagreb*

Abstract: Circular γ polarization in heavy nuclei (Ta^{181}, Lu^{175}) has been calculated using the two-body parity-nonconserving potential deduced on the basis of several weak-interaction Hamiltonians. Gauge invariance was elucidated by the Feynman-diagram analysis. The relative contributions from various nuclear single-particle states have been analyzed in detail. Short-range correlations have been approximately taken into account. Our calculation is compared with earlier calculations. According to our calculations, the Cabibbo conventional weak-Hamiltonian model seems to disagree with the Ta^{181} experiment. Other models allowing for extra neutral currents, such as d'Espagnat and the Lee model, might agree with experimental results. This conclusion depends on the sign of the theoretical result, which cannot be fixed with absolute certainty. The Oakes model seems to give absolute values which are too large.

* Work publiched in Fizika 4 (1972) 97-111

**Published in Physical Review C 4 (1971) 661—672.

5.4. The complete interpretation of data from gamma-skip-gamma directional correlation measurements — ^{124}Te

A. H. KUKOČ, R. B. VUKANOVIĆ and I. V. ANIČIN, *Institute »Boris Kidrič«, Beograd*

5.5. Time coincidences in the reactions Er(n, γ) and Lu(n, γ)

J. SIMIĆ, S. KOIČKI and B. LALOVIĆ, *Institute »Boris Kidrič«, Beograd*

5.6. Linear polarization of 662 and 279 keV gamma rays elastically scattered in uranium

B. MOLAK, J. NOSIL and K. ILAKOVAC, *Institute »Ruđer Bošković«, Zagreb*

The measurements were performed in an arrangement described in Ref.[1] A planar Ge(Li) detector of $\phi 18 \times 3$ mm was used as a polarization analyzer. The scatterer was a disc of uranium metal of $\phi 32 \times 10$ mm. The gamma ray sources, ^{137}Cs of 5 Ci or ^{203}Hg of about 1 Ci, were placed inside a heavy lead shield. The shield and the scatterer were mounted inside a steel cylinder. The cylinder was pivoted in a fork to change the scattering angle, and the fork was mounted onto a shaft to rotate the scattering plane (sce Fig).

Small deviations of the detector from the axis of rotation cause considerable changes in the counting rate due to the strong dependence of the cross sections on the scattering angle. However, the change of the sum of counting rates at two

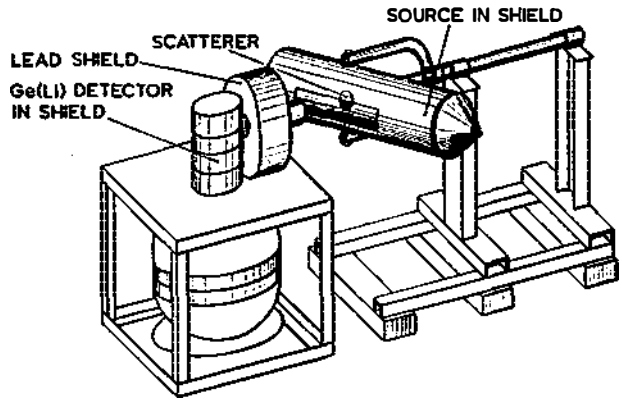

Fig.

opposite positions of the source cancels to first order, and in this way systematic errors can be practically eliminated. Therefore, the counting rates for both the »parallel« (N_1) and the »perpendicular« (N_2) orientation of the polarization plane with respect to the detector were determined for two opposite positions of the source (four positions altogether).

From the measured counting rates the asymmetry $A = (N_1 - N_2)/(N_1 + N_2)$ was determined. The polarimetric efficiency ε of the analyzer was calibrated by measuring the asymmetry in Compton scattering. From the relation $P = A/\varepsilon$ the degree of linear polarization was determined.

TABLE 1

Linear polarization in elastic scattering of 662 keV gamma rays
$Z = 92$ $\varepsilon = 6.54 \pm 0.95$

Θ	51°	60°	75°	90°	105°	120°	135°
$-A(\%)$	3.14±0.36	4.75±0.42	6.55±0.68	3.74±0.50	1.85±0.66	2.14±0.66	0.67±0.83
$-P(\%)$	48.8±9.0	72.5±12.4	100.2±15.0	57.1±11.3	28.3±11.0	32.7±10.9	10.2±12.6
$-P(\%)^*_{\text{theor}}$	60.0	82.8	99.0	78.5	48.0	25.3	12.0

* theoretical results of Ref.[2] for $Z = 82$ and $E_\gamma = 654$ keV.

TABLE 2

Linear polarization in elastic scattering of 279 keV gamma rays
$Z = 92$ $\varepsilon = 4.59 \pm 0.14$ ($E_\gamma = 288$ keV)

Θ	45°	60°	75°	90°	105°	120°	135°
$-A(\%)$	2.03±0.48	—	3.8±0.6	4.15±0.83	3.6±0.9	—	1.45±0.57
$-P(\%)$	44.3±10.6	—	82.7±13.4	90.5±18.3	78.4±19.7	—	31.7±12.4
$-P(\%)^*_{\text{theor}}$	43	75	85	94	68	38	20

* theoretical results of Ref. [2] for $Z = 82$ and $E_\gamma = 327$ keV.

The results of measurements with 662 keV and 279 keV gamma rays are shown in Table 1 and Table 2, respectively. The tables also show the theoretical results of Ref.[1] for scattering in mercury at energies of 654 keV and 327 keV, respectively.

References

1) B. Molak, K. Ilakovac and J. Nosil, this issue p. 15;
2) G. E. Brown and D. F. Mayers, Proc. Roy. Soc. A234 (1956) 387; A242 (1957) 89.

5.7. Internal and external double-electron ejection

K. PISK and K. ILAKOVAC, *Institute »Ruđer Bošković«, Zagreb*

Processes of double electron ejection from an atom due to the absorption of a real or virtual photon have been considered. The amplitudes of the processes consist mainly of two coherent parts: the »shake-off« and the »direct collision« amplitude[1]. In the absorption of a virtual photon (e. g. decay of a nuclear excited state) a second order transition[2] is also possible, but the contribution of this process is usually negligible[3]. The shake-off and the direct collision amplitude were calculated by Feinberg[4] for the internal ionization in beta decay. Porter et al.[5] applied those results for an estimate of internal ionization in K-conversion.

In this paper our calculations of the direct collision amplitudes of the internal and external double electron ejection are discussed. The impulse approximation[6] was applied, i. e. the nuclear Coulomb field was taken into account only through the wave functions of bound electrons. Feynman diagram techniques were used to calculate the amplitudes of transitions.

In the case of absorption of a real photon (double-electron photoelectric effect), the differential cross sections $d\sigma/d\Omega_1 d\Omega_2 dT$ were calculated. Since three particles are in the final state, the directions of emission $d\Omega_1$ and $d\Omega_2$ of the electrons are independent and the energy of one electron T is continuously distributed. A helium-like atom of nuclear charge Ze was assumed and the mutual perturbation of the two electrons neglected (before the absorption of the photon). The calculated energy distributions of electrons are generally double peaked. The cross sections integrated over the energy increase with increasing Z and decresing energy of incident photons, and show a strong dependence on linear polarization (the scattering is mainly in the plane of polarization).

A multipole expansion of the interaction between K electrons and the nucleus was made in the calculations of the direct collision process in internal ionization in K conversion. Coulomb interaction in the electron-electron collision was assumed. Only magnetic type transitions of the nucleus were considered. For the double — K electron ejection process the differential probabilities $dw(\Theta)/d\Omega dT$ were calculated, where Θ is the angle of relative emission of the electrons and T the energy of an electron. The same approximations were applied in the calculations of the K conversion for the same nucleus, energy of transition and multipolarity. The ratio of probabilities for the KK process integrated over the energy or over the solid angle and of the K-conversion transition probabilities was calculated for comparison with experimental measurements.

References

1) R. L. Intemann and F. Pollock, Phys. Rev. **157** (1967) 41;
2) J. Eichler, Z. Physik **160** (1960) 333;
3) A. Ljubičić, M. Jurčević, K. Ilakovac and B. Hrastnik, Phys. Rev. **3C** (1971) 831;
4) E. L. Feinberg, Jadern. Fiz. **1** (1965) 612;
5) F. T. Porter, M. S. Freedman and F. Wagner, Jr., Phys. Rev. **3C** (1971) 2246;
6) J. Waller and D. R. Hartree, Proc. Roy. Soc. **A29** (1928) 119.

5.8. Measurement of the gamma transition intensities in ^{185}Re

Đ. M. KURBANI, M. STANOJEVIĆ and M. BOGDANOVIĆ, *Institute »Boris Kidrič«, Beograd*

5.9. Search for the $\gamma\gamma$ decay of the 392-keV state in ^{113}In

K. ILAKOVAC, B. MOLAK and M. JURČEVIĆ, *Institute »Ruđer Bošković«, Zagreb*

An attempt to observe the double-gamma decay of the 1.7^h isomeric state of ^{113}In was made. A source of ^{113}Sn of about 60 μCi was used. Two coaxial Ge(Li) detectors of 17 cm^3 and 20 cm^3 detected photons emitted from the source at a relative angle of about 90°. Coincident events were analyzed in a fast coincidence system and a 128 × 256 × 256 channel three-dimensional analyzer. The time difference was measured by means of a time-to-amplitude converter and recorded in the first channel, and the amplitude of pulses from the two detectors were recorded in the other two channels. The 3D analyzer uses punched paper tape for the recording of data, and the tape is analyzed off-line in a CAE 9040 computer.

Energy and timing calibration were made by Compton scattering of 392-keV gamma rays from one detector into the other. By varying the scattering angle it was possible to change the fraction of energy released (to the Compton recoil electron) in the first detector, the rest being carried by the secondary Compton photon to the second detector. The timing (except for a negligible delay due to different distances) and the energy relations are the same as in the double gamma decay of the 392-keV state in ^{113}In.

The analysis of data has not been completed. A preliminary result for the ratio of the transition probability of gamma-gamma decay and of single gamma-ray emission, assuming an isotropic angular distribution, has been obtained:

$$T_{\gamma\gamma}/T_{\gamma} < 2 \cdot 10^{-5}$$

This result is to be compared with the single-particle theoretical estimate[1] of $1.6 \cdot 10^{-6}$.

Reference

1) D. P. Grechukhin, Nucl. Phys. **62** (1965) 273.

5.10. Z-dependence of linear polarization in Rayleigh scattering

N. BILIĆ, M. MARTINIS and K. PISK, *Institute »Ruđer Bošković«, Zagreb*

In the experiment of B. Molak et al.[1] it was shown that the degree of linear polarization in Rayleigh scattering decreases with increasing Z at 90°. The energy of gamma rays was 662 keV. The exact numerical approach of Brown et al.[2] would involve great computational dificulties. Since polarization is simply the ratio between cross sections, we are able to obtain the Z-dependence of linear polarization in a more direct way by taking into account the following approximations:

a) the contribution to Rayleigh scattering is essentially by K-shell electrons[2];

b) the energies of gamma rays are much larger than the binding energy of K electrons. It is therefore possible, at least in the second order perturbation theory, to use the free electron propagator instead of a large number of intermediate states which would have to be taken into account in the exact calculation. (This approximation is known as the impulse approximation[3].)

c) The wave function of the K electron is taken in the lowest order in $Z\alpha$ (Ref.[4]), and the effect of other electrons is neglected.

Taking into account a), b) and c) we obtain the following form for the Rayleigh scattering amplitude by K-shell electrons

$$A \sim \int \mathrm{d}^3 p \begin{pmatrix} 2m\Phi(\vec{p}')w \\ -\Phi(p')\vec{\sigma}\cdot\vec{p}'w \end{pmatrix}^{+} \gamma_0 \left[\hat{e}_2 \frac{\mathrm{i}f_1 - m}{f_1^2 + m^2} \hat{e}_1 + \hat{e}_1 \frac{\mathrm{i}f_2 - m}{f_2^2 + m^2} \hat{e}_2 \right] \begin{pmatrix} 2m\Phi(\vec{p})w \\ -\Phi(\vec{p})\vec{\sigma}\cdot\vec{p}w \end{pmatrix}$$

If we drop the small components in the above relation we obtain the classical result in which the Z-dependence disappears[5].

In a rather rough estimate the above amplitude gives a simple analytical expression for polarization P at 90°,

$$P = \frac{1 - \frac{1}{4}\left[\left(\frac{\varepsilon_\gamma}{m}\right)^2 + \frac{1.8\,(Z\alpha)^2}{[1 + (1 - Z\alpha)^2]}\right]}{1 + \frac{1}{4}\left[\left(\frac{\varepsilon_\gamma}{m}\right)^2 + \frac{1.8\,(Z\alpha)^2}{[1 + (1 - Z\alpha)^2]}\right]},$$

where ε_γ is the photon energy, m the mass of the electron, Z the nuclear charge, and $\alpha = 1/137$ the fine structure constant.

Comparison with the experimental data[1] and the calculation of Brown et al.[2] is quite good, having in mind the roughness of the approximation.

References

1) B. Molak, K. Ilakovac and A. Ljubičić, Fizika 3 (1971) 239;
2) G. E. Brown, R. E. Peierls, F. R. S. and J. B. Woodward, Proc. Roy. Soc. **A227** (1955) 51;
S. Brenner, G. E. Brown and J. B. Woodward, Proc. Roy. Soc. **A227** (1955) 59;
G. E. Brown and D. F. Mayers, Proc. Roy. Soc. **A234** (1956) 387;
G. E. Brown and D. F. Mayers, Proc. Roy. Soc. **A242** (1957) 89;
3) J. Waller and D. R. Hartree, Proc. Roy. Soc. **A24** (1928) 119;
4) H. A. Olsen, Springer Tracts in Modern Physics, 44;
5) W. Franz, Z. Physik **95** (1935) 652; **98** (1936) 314.

5.11. The EO component in the $2^+ - 2^+$ transition of 879 keV in the ^{160}Dy

M. ŽUPANČIĆ, I. BIKIT and L. MARINKOV, *Institut of nuclear sciences »Boris Kidrič«, Beograd*

The analysis of the $2^+ - 2^+$ transition in the ^{160}Dy is the continuation of a systematic work done by authors in the last few years[1-5]. Electron-gamma directional correlation measurement of the 2^+(879 keV)2^+(87 keV)0^+ cascade have been made. The electric monopole to quadrupole mixing ratio q_k for the 879 keV

transition was determined. Under the assumption that there are no penetration effects result is:

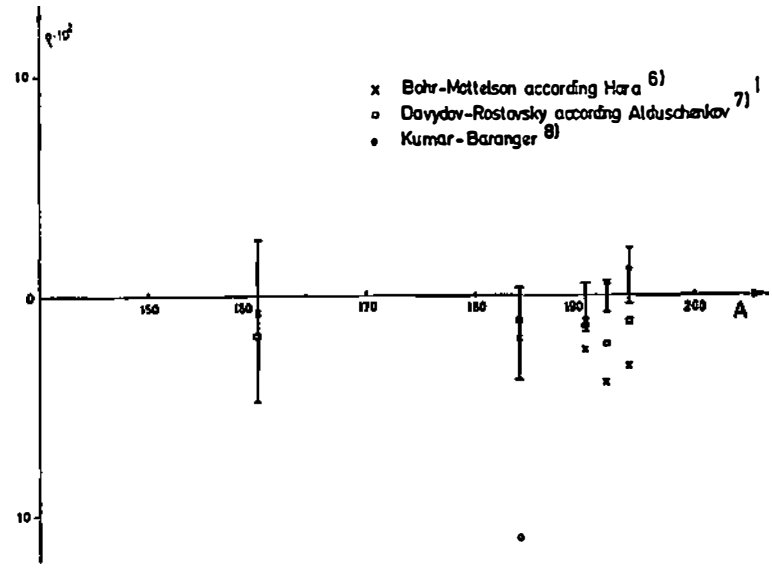

Fig. 1. The ϱ values for the $2^+ \rightarrow 2^+$ transitions of 879 keV in the ^{160}Dy, 793 keV in the ^{184}W[2], 371 keV in the ^{190}Os[4], 296 keV in the ^{192}Pt[3] and 293 keV in the ^{194}Pt[5], compared with some theoretical predictions.

$$q_k = -0.03(10)$$

From that value the reduced matrix element of the EO transition ϱ was calculated. On the Fig. 1 our value of ϱ together with the results from the ref[2,3,4,5] are compared with some theoretical predictions.

References

1) M. Župančić, R. Vukanović, L. Marinkov and D. Krmpotić, Radioactivity in Nuclear spectroscopy, ed. J. H. Hamilton, J. C. Manthuruthil, Gordon and Breach (in press);
2) M. Župančić, R. Vukanović and L. Samuelsson, Ark. Fys. **39** (1969) 313;
3. L. Marinkov, I. Aničin, I. Bikit and R. Stepić, Nucl. Phys. **A131** (1969) 601;
4) L. Samuelsson, R. Vukanović, M. Migahed, M. Župančić, L. O. Edvardson and L. Westerberg, Nucl. Phys. **A135** (1969) 657;
5) D. M. Krmpotić, L. G. Marinkov and A. H. Kukoč, Fizika **1** Suppl. 1 (1969) 49;
6) K. Hara, Nucl. Phys. **46** (1963) 385;
7) A. V. Alduschenkov and N. A. Voinova, Akad. Nauk. SSSR Phys. Teh. Inst. A. F. Ioffe **319** (1971);
8) K. Kumar and M. Baranger, Nucl. Phys. **A122** (1968) 273.

FIZIKA 4 Suppl. (1972)

SECTION 6 — NUCLEAR REACTIONS AND CAPTURE PROCESSES

6.1. Prompt γ-ray spectra and integrated cross sections for the radiative capture of 14 MeV neutrons

F. CVELBAR, M. BUDNAR and M. POTOKAR, *J. Stefan Institute and Faculty for Natural Sciences and Technology, University of Ljubljana*

Introduction. The excitation energy E of the intermediate system after capture of neutrons of the energy between 5 MeV and 10 MeV is between about 12 MeV and 22 MeV i. e. in the region of the giant dipole resonance (GDR). In this region the dipole absorption of γ-rays is enhanced. On the other hand the nuclei, being excited e. g. just to the peak energy $E = E_R$ of GDR should have enhanced probability for dipole deexcitation to the ground state.

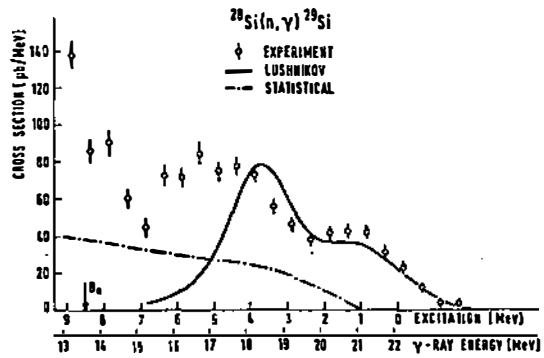

Fig. 1. Spectrum of prompt γ-rays from the radiative capture of 14,1 MeV neutrons in ^{28}Si.

According to the collective (semi-direct) model[1] this is a consequence of the fact that a part of the wave function of such an intermediate state can be written as a product of the wave function, describing the collective dipole vibrations and the ground state wave function.

If the excitation energy is higher than E_R and appears as a sum $E = R_R + E_f$, where E_f means the energy of one of the bound states, in the above product, the wave function of this state appears instead of the ground state wave function.

Correspondingly the maximum spectral intensity is not expected to be found in the ground state transition but in the transition to the excited state.

When the excitation energy cannot be divided exactly into a sum of E_R and E_f but $E = E'_R + E_f$ where E'_R is an energy not exactly equal to the peak value of the GDR but still within its width, for the transitions to the different final states the previous expectation applies, except that the intensity is reduced due to the fact that $E'_R \neq E_R$.

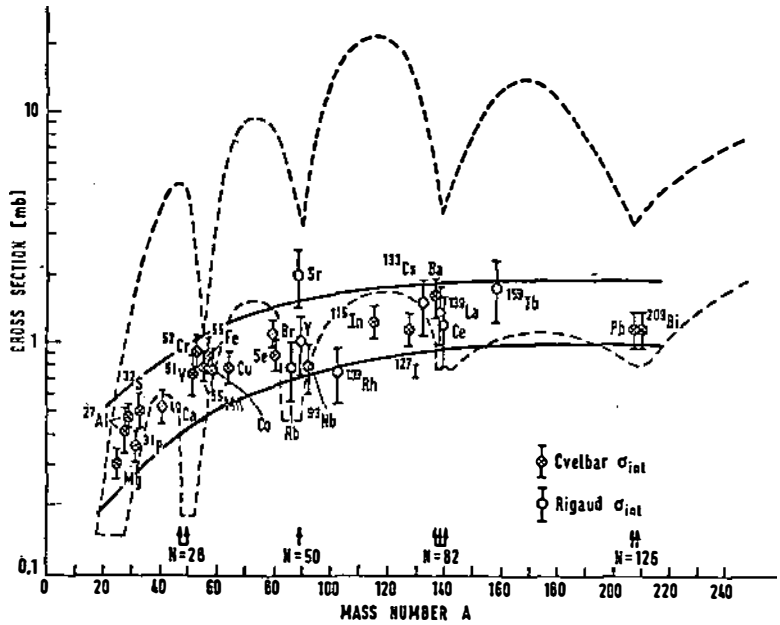

Fig. 2. Mass dependence of the integrated cross section for the radiative capture of 14 MeV neutrons. Corresponding activation cross section values are scattered within the region bounded by the broken line.

From this it follows that in the spectra from the radiative capture of 14 MeV neutrons the shape of the GDR should be in some way reproduced. This expectation was confirmed experimentally in many cases (see e. g. Refs.[2,3]).

Results. Prompt γ-ray spectra from the radiative capture of 14,1 MeV neutrons such as the one presented in Fig. 1 were measured in this laboratory with a special telescopic scintillation pair spectrometer which allows the measurement of γ-rays from a sample placed around the neutron source. Spectra obtained in this way are integrated over 4π solid angle and are therefore directly comparable with the calculated ones[2,3] without knowledge or speculation about the angular distribution of γ-rays from the capture process. In Fig. 1 the experimental γ-ray spectrum for ^{28}Si is compared with the result of the calculation according to the approach of Lushnikov and Zaretsky.

The integrals of the measured (n, γ) spectra (σ_{int}) have been compared with the values (σ_{act}) obtained by the activation technique[4]. As the values of σ_{int} cover only the transitions to the bound states of final nuclei, but the σ_{act} include also the transitions via unbound states, it was expected that $\sigma_{act} > \sigma_{int}$. The difference

should be of the order of a few tens of percent. The probability of populating unbound states by radiative transitions is reduced by the factor E^3 (dipole term in multipole expansion), but the probability for further γ-ray deexcitation is additionally reduced due to the high probability of particle emission.

The experimentally observed values of σ_{act} are up to 20 times higher than the σ_{int}. In contrast with the σ_{int}, which shows a smooth mass dependence saturating in the region of medium nuclei where the cross section is about 1,2 mb, the values of σ_{act} are scattered between 0,5 mb and 20 mb. The two cross sections roughly agree only for nuclei in the vicinity of closed neutron shells. Probably the most convincing explanation for this discrepancy is that based on the suposition that the σ_{act} observations are severely contaminated by events due to the slowed down neutrons (for which the capture cross sections tend to be larger). This conjecture is supported by the similarity of the observed A dependence of σ_{act} for 1 MeV and 14 MeV neutrons, i. e. both show the same extreme dependence on shell structure.

References

1) J. Zimanyi, I. Halpern and V. A. Madsen, Phys. Lett. **33B** (1970) 205 and references citied therein;
2) F. Cvelbar, A. Hudoklin, M. V. Mihailovič, M. Najžer and M. Petrišič, Nucl. Phys. **A130** (1969);
3) F. Cvelbar and A. Hudoklin, Nucl. Phys. **A159** (1970) 555;
4) F. Cvelbar, A. Hudoklin and M. Potokar, Nucl. Phys. **A158** (1970) 251.

6.2. The radiative capture of 10 MeV neutrons in heavy nuclei

M. POTOKAR, F. CVELBAR and M. BUDNAR, *J. Stefan Institute, and Faculty for Natural Sciences and Technology, University of Ljubljana*

In an attempt to remove considerable discrepancies between the early experimental data on fast (10—30 MeV) nucleon capture and the predictions of the statistical theory and the simple direct theory of nucleon capture the so-called direct-semi direct (DSD) theory arose. The spectra of prompt gamma-rays following the radiative capture of 14 MeV neutrons have been recognized as an effective tool for testing the new theory. The agreement between the experimental spectra and the spectra calculated by using this theory has been good in the case of light and medium nuclei[1]. The integrated cross sections obtained by summing all counts in the spectrum corresponding to gamma-ray transitions to bound states have been found to exhibit smooth mass dependence, the cross sections being between 300 μb and 1200 μb, increasing with A. This observation is in contradiction with the cross section data obtained by the activation technique, but does not contradict DSD theory[2].

The investigation of the capture process has now been extended to the heavy nuylei. The experimental spectra of Ba, Pb and Bi are presented for the first time. These spectra are reasonably reproduced by the theory, so confirming at least the general correctness of the present day state of DSD theory for the radiative

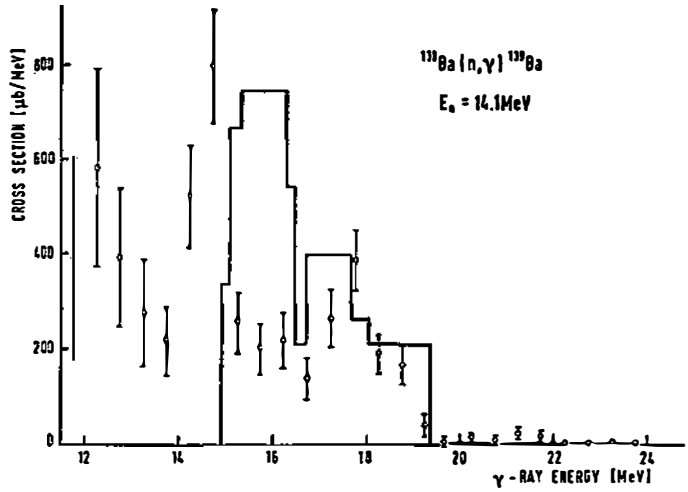

Fig. 1 Comparison of experimental (circles) and theoretical (solid line) spectrum of γ-rays from the radiative capture of 14,1 MeV neutrons in barium.

capture process. Fig. 1 presents the measured spectrum for ^{138}Ba in comparison with the spectrum calculated according to Zimanyi, Halpern, and Madsen formulation[3] of DSD theory. The integrated cross sections agree with our previously found smooth mass dependence, the values being 1600 ± 300 μb, 1150 ± 200 μb, and 1150 ± 200 μb for Ba, Pb and Bi, respectively.

References

1) F. Cvelbar, A. Hudoklin, M. V. Mihailović, M. Najžer and M. Petrišič, Nucl. Phys. **A130** (1969) 413;
2) F. Cvelbar, A. Hudoklin and M. Potokar, Nucl. Phys. **A158** (1970) 251 (other references contained therein);
3) J. Zimanyi, I. Halpern and V. A. Madsen, Phys. Lett. **33B** (1970) 205.

6.3. ^{9}Be(^{3}He, p)^{11}B reaction at low ^{3}He energy

D. M. STANOJEVIĆ, K. M. SUBOTIĆ, B. Z. STEPANČIĆ, R. V. POPIĆ and M. R. ALEKSIĆ, *Institute of nuclear sciences »Boris Kidrič«, Beograd*

We report on the measurements of excitation functions for twelve groups of protons emerging from the reaction ^{9}Be(^{3}He, p)^{11}B for $0.5 < E_{^{3}\mathrm{He}} < 1.1$ MeV. This energy region corresponds to the excitation of ^{12}C nucleus from 26.78 up to 27.38 MeV where the data on ^{12}C are scarse and inadequate. From the reaction

$^{11}B(p, \gamma)^{12}C$ there is an indication[1] on the existence of a resonance corresponding to a level of ^{12}C at 26.9 MeV, which possibly might be seen in $^{9}Be(^{3}He, p)^{11}B$ reaction at $E_{^3He} \approx 0.82$ MeV.

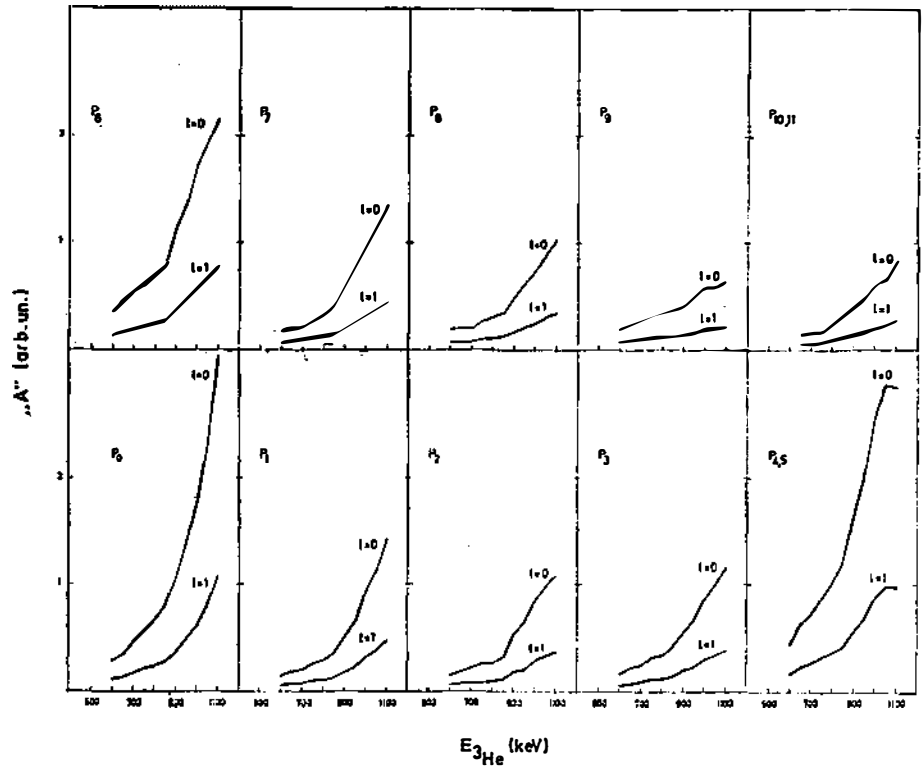

Fig. 1. 110° excitation functions for $^{9}Be(^{3}He, p_{0-11})^{11}B$.

The analyzed ^{3}He beam was obtained from the 1.5 MeV Cockcroft-Walton accelerator of the »Boris Kidrič« Institute. The target was metallic Be evaporated onto a thin Al foil. A Si-detector, 2 mm thick, was used for the detection of protons. Ten peaks in proton spectrum belong to twelve proton groups, two peaks being doublets (p_4, p_5 and p_{10}, p_{11}). The excitations of all ten peaks are given in Fig. 1.

It is typical that all ten excitation functions are free from any resonant behaviour. Since the Coulomb barrier strongly dominates the behaviour of excitation curves at low energy, we have computed the quantity;

$$A = \frac{N_{exp}}{4\frac{k_{out}}{k_{in}} P_{l_{in}} P_{l_{out}}}$$

where N_{exp} is the c. m. yield taken from our excitation curves, k_{in} belongs to ^{3}He and k_{out} to proton groups, while $P_{l_{in}}$ and $P_{l_{out}}$ are Coulomb barrier penetration factors for incoming and outgoing channels. The quantity A, computed for each

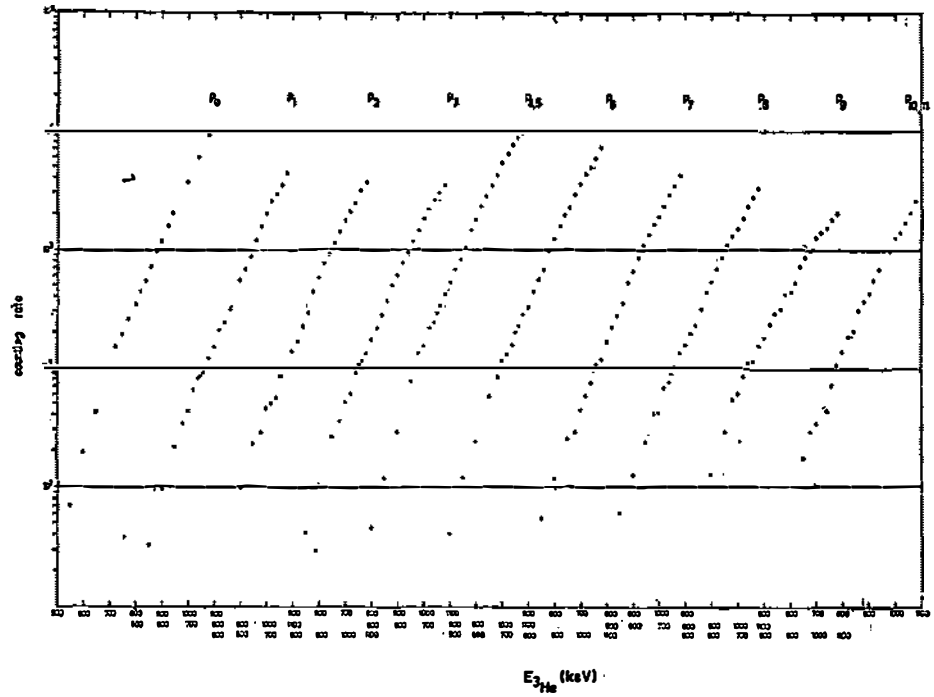

Fig. 2. Quantity A_0 computed for $l = 0$ and $l = 1$.

proton group separately, is given in Fig. 2. This additional analysis did not show any resonant structure too. Therefore, it seems reasonable to conclude that the $^9Be(^3He, p_{0-11})^{11}B$ reaction, even at low energy, proceeds via a direct process.

Reference

1) F. Ajzenberg-Selove and T. Lauritsen, Nucl. Phys. **A114** (1968) 44.

6.4. $^9Be(^3He, n)^{11}C$ reaction between 600 and 1100 keV

K. SUBOTIĆ, R. POPIĆ, D. STANOJEVIĆ, B. STEPANČIĆ and M. ALEKSIĆ, *Institute of nuclear sciences »Boris Kidrič«, Beograd*

The cross-section of $^9Be(^3He, n)^{11}C$ reaction, determined for all neutron groups together by measuring β^+ decay of the residual ^{11}C, rises from 0.1 mb at $E_{^3He} = 600$ keV to 8 mb at $E_{^3He} = 1150$ keV. The data for the individual neutron groups are obtained by measuring the gamma spectra from ^{11}C, which were analysed and resolved in order to correspond to the different gamma transitions in ^{11}C.

6.5. A check of the existence of the ternary fission of ^{235}U induced by thermal neutrons

R. ANTANASIJEVIĆ, M. JURIĆ and V. GERC, *Institute of Physics, Beograd*

An investigation of the ternary fission of ^{235}U has been carried out with nuclear emulsions and solid state track detectors sensitive to particles of $A > 4$ and $A > 16$. The uranium target was homogeneously distributed throughout the emulsion, or vacuum evaporated on the two foils of the solid state detector (polycarbonate). In the solid state detector, the following three types of events have been found:

a) events with two collinear tracks (binary fission),
b) events with two tracks making an angle less than 180° and
c) events with three tracks.

Events b) and c) may be accidental (T^-), due to coincidence of binary events, and T^+, which represent cases of binary fission fragments scattering on target and detector nuclei, or ternary fission.

A computer program has been devised to calculate all elements of T^+ events and to discriminate cases of scattering from the ternary fission. On the basis of this a comparison is made of the results obtained by means of the two detectors. The yield of ternary fission relative to binary fission is determined.

6.6. Activation measurements of fast neutron radiative capture

R. ČAPLAR, E. HOLUB, P. KULIŠIĆ, Đ. VESELIĆ and N. CINDRO, *Institute »Ruđer Bošković«, Zagreb*

J. VULETIN, *Faculty of Electrical Engineering, Split*

The existing differences in fast neutron capture cross sections obtained by the activation[1,2] and integration methods[3,4] are presently the subject of considerable interest. In principle, σ_{int} should be smaller than σ_{act}, since the former quantity measures only the decay to the bound states of the final nucleus (target + neutron), i. e. the prompt gamma spectra, while the latter includes the decays to the bound and the unbound states. However, this difference should not be too large, since the decay to the unbound states leads normally to the emission of particles and gamma rays compete favourably with particle emission only in the region just around the binding energy where the available neutron energy might be too small to overcome the centripetal barrier.

As the present experimental evidence shows (Fig. 1), the integration cross sections follow a smooth path. The activation cross sections vary considerably as a function of A, but also σ_{act} measured by different authors yield results which differ by more than a factor of two (see, e. g. the case of ^{127}I in the Table).

For all these reasons and unanswered questions our group in Zagreb started a systematic survey of 14 MeV (n, γ) reactions by the activation method. A standard Ge(Li) detector of 20 cm^3 active volume in connection with a 256-channel analyser was used. At the beginning we measured (n, γ) cross sections on ^{23}Na, ^{27}Al, ^{37}Cl, ^{55}Mn, ^{41}K and ^{127}I. For ^{37}Cl it is the first measurement of σ_{act} around 14 MeV.

The results are shown in the Table. The reactions $^{56}Fe(n, p)$, $^{27}Al(n, p)$ and $^{27}Al(n, \alpha)$ were used as monitoring reactions. Corrections were made for nonpoint geometry. We also used samples, such as $FeCl_3 \times 6H_2O$, where both the reaction in question and the monitoring reaction were simultaneously induced. This, then, eliminated geometrical corrections.

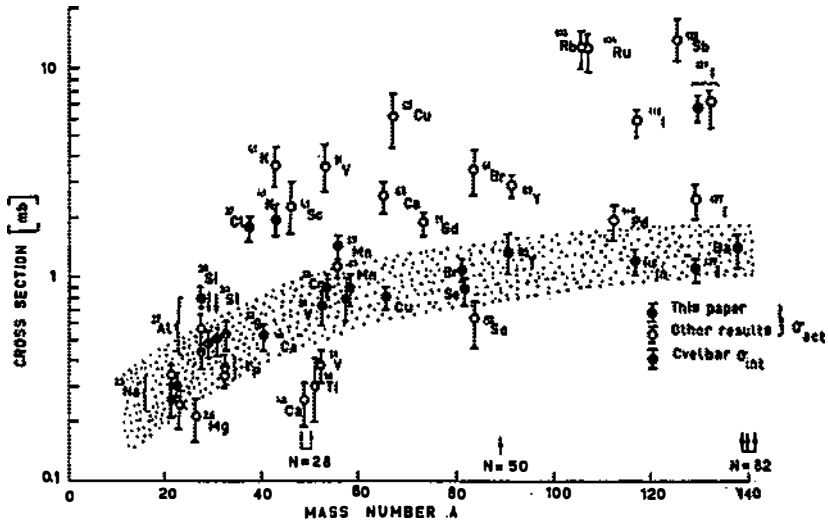

Fig. 1.

The obtained results show a difference in behaviour of σ_{act} and σ_{int} by varying the number A. σ_{act} appears to be always larger than σ_{int}. This difference is small around the closed neutron shells, but the difference between the closed neutron shells could be as large as an order of magnitude.

TABLE

Isotope	Sample	Activation cross section		Ref.
		this paper (mb)	others (mb)	
^{23}Na	NaCl	0.25±0.04	0.24±0.06 0.33±0.03	1) 7)
^{27}Al	Al natural	0.8±0.1	0.56±0.10	1)
^{37}Cl	NaCl $FeCl_3 \times 6H_2O$	1.8±0.2		
^{55}Mn	MnO_2	1.4±0.2	1.2 ±0.3 0.76±0.08	1) 7)
^{41}K	KIO_3	2.0±0.3	3.5±0.7	7)
^{127}I	KIO_3	7.0±0.5	7.2±1.2 2.5±0.5	6) 7)

A possible explanation is that activation measurements are influenced by the presence of ~1 MeV neutrons produced by the (n, 2n) reaction in the target. Preliminary calculations[5], made for holmium indicate that up to 25% of the measured activation could be accounted for by this interpretation. It is not likely that reactions of the type (n, nX) could explain the rest of the order of magnitude difference between σ_{act} and σ_{int}.

Our results thus present the beginning of a systematic measurement of 14 MeV (n, γ) cross sections by the activation method with the double aim to reduce the scattering of various experimental results and to look for the systematic differences with σ_{int}. So far the results in the $d_{3/2} - f_{7/2}$ region have confirmed the earlier prediction in the sense that σ_{act} is consistently larger than σ_{int}.

References

1) I. Csikai, G. Petö, M. Buczkó, Z. Miligy and N. A. Eissa, Nucl. Phys. **A95** (1967) 229;
2) P. N. Tiwari and E. Kondaiach, Phys. Rev. **167** (1968) 1091;
3) F. Cvelbar, A. Hudoklin, M. V. Mihailović, M. Najžer and V. Ramšak, Nucl. Phys. **A130** (1969) 401;
4) F. Cvelbar, A. Hudoklin und M. Potokar, Nucl. Phys. **A158** (1970) 251;
5) F. Rigaud, J. L. Irigaray, G. Y. Petit, G. Longo and F. Saporetti, Nucl. Phys. **A176** (1971) 545;
6) S. M. Qaim and M. Ejaz, Journal of Inorganic and Nuclear Chemistry **30** (1968) 2577;
7) I. L. Perkin, L. P. O'Conner and R. F. Coleman, Proc. Phys. Soc. **72** (1958) 505.

6.7. Isomeric cross section ratios for (n, p) reactions induced by 14.6 MeV neutrons in Te isotopes

S. LULIĆ and M. DIKŠIĆ, *Institute »Ruđer Bošković«, Zagreb*

Introduction. Measurement of the ratio of the yield of isomeric pairs as a function of energy is a useful tool for the investigation of the mechanisms of the nuclear reactions. Huizenga and Vandenboch[1] have developed a method for calculating the theoretical isomeric ratio in (x, n) reactions on the basis of the statistical theory.

Although the isomerism in isotopes of tellurium is well established, the available data on the yield ratio for the isomeric pair formation of tellurium isotopes is surprisingly small, particularly for the 14—15 MeV neutrons. In this work we have measured the (n, p) cross sections for the metastable and ground states of all unstable tellurium isotopes. The choice was, moreover, influenced by the desire to investigate further the effect known from the works of Levkovski[2,3], Gardner[4] and others[5,6,7,8]. This effect consists in a regular decrease of the (n, p) cross sections of isotopes of the same element with the increase of the mass number.

Experimental. Natural tellurium was used in the form of chemically pure and specpure powders. Enriched ^{120,122,124,126,128,130}Te used in the work were obtained from the Oak Ridge National Laboratory, Oak Ridge, Tennessee.

Irradiations were performed at 14.6 ± 0.2 MeV with neutrons obtained from the $^2H + ^3H$ reaction using 200 keV Cockcroft-Walton generator of the Institute »Ruđer Bošković«. The neutron flux was about 2×10^9n/sec, and the total neutron yield was monitored by the associated α-particles. The duration of irradiation time was varied from several minutes to several hours depending on the half-live of the products. Gamma-ray spectra were measured using 25 cm^3 Ge(Li) detector coupled to the 400-channels analyser.

TABLE

Target	Product	Exp. val. (mb)	σ_m/σ_g	Theoretical values									
				$\sigma = 3$ or 4					$\sigma = 7$				
				ν					ν				
				1	2	3	4	5	1	2	3	4	5
^{120}Te	^{120m}Sb	64±10	0.78	.241	.243	.247	.251	.273	.505	.584	.588	.669	.722
	^{120g}Sb	82±13											
^{122}Te	^{122m}Sb	21±6	0.81	.120	.130	.138	.144	.148	.302	.364	.422	.473	.519
	^{122g}Sb	17±3											
^{124}Te	^{124m1}Sb	5±0.8	0.38	.830	.870	.882	.923	.949	.644	.648	.638	.637	.632
	^{124m2}Sb	2±0.3											
	^{124g}Sb	13±2	0.15	.272	.337	.386	.434	.475	.159	.172	.179	.183	.185
^{126}Te	^{126m}Sb	1.5±0.1	0.50	.177	.212	.240	.268	.286	.262	.328	.376	.423	.466
	^{126g}Sb	3±0.9											
^{128}Te	^{128m}Sb	1±0.1	0.67	—	—	—	—	—	—	—	—	—	—
	^{128g}Sb	1.5±0.3											
^{130}Te	^{130m}Sb	0.9±0.2	0.64	—	—	—	—	—	—	—	—	—	—
	^{130g}Sb	1.4±0.3											

for 126 Te $\sigma = 3$

Results. In the Table the experimental and theoretical isomeric ratios for (n, p) reactions are shown. Calculations of the isomeric ratio were performed for several values of ν ($\nu = 1, 2, 3, 4, 5$) and for several vaues of the cut-off parameter σ ($\sigma = 3, 4, 7$) included in the known formula for spin-dependent level density[9]:

$$\varrho(J) \propto \varrho(0)(2J + 1)\exp[-(J + 1/2)^2/2\sigma^2]$$

The calculations are based on the theory of the reactions occurring through the compound nucleus.

Our measured values for isomeric ratio are in reasonable agreement with the previously measured values of Husain and Kuroda[10], but in complete disagreement with Brzosko et al.[11].

References

1) J. R. Huizenga and R. Vandenboch, Phys. Rev. **120** (1960) 1305;
2) V. N. Levkovskii, JETP **31** (1956) 360;
3) V. N. Levkovskii, JETP **33** (1957) 1520;
4) D. G. Gardner, Nucl. Phys. **29** (1962) 373;
5) R. J. Wille and R. N. Fink, Phys. Rev. **118** (1960) 242;
6) J. M. Ferguson and W. E. Thomson, Phys. Rev. **118** (1960) 228;
7) F. L. Preiss and R. W. Fink, Nucl. Phys. **15** (1960) 326;

8) S. Lulić et al., Nucl. Phys. **A119** (1968) 517;
9) C. Bloch, Phys. Rev. **93** (1954) 1094;
10) L. Husain and P. K. Kuroda, Nucl. Phys. **A114** (1968) 663;
11) J. Brzosko et al., Nucl. Phys. **45** (1963) 579.

6.8. The distortion of the deuteron by the Coulomb field*

E. COFFOU, *Institute »Ruđer Bošković«, Zagreb*

* Work published in Fizika 4 (1972) 141.

CONTENTS

SECTION 3 — Nuclear structure

SECTION 4 — Simple particle systems

SECTION 5 — Nuclear Spectroscopy

SECTION 6 — Nuclear reactions and capture processes

Tisak: Grafički zavod Hrvatske, Zagreb, 1973.